

DRAFT

**Texas Commission on Environmental Quality
Service Order 18**

Contract No. 582-4-56385

AIR POLLUTANT CONCENTRATIONS NEAR TEXAS ROADWAYS

August 31, 2007

DRAFT FINAL REPORT

Submitted to

**Valerie Meyers, Ph.D.
Texas Commission on Environmental Quality
Chief Engineer's Office
Toxicology Section
Austin, TX**

Submitted by

**David Allen*, Allison DenBleyker, Edward Michel,
Yifang Zhu, Matt Fraser, Donald Collins, and Elena McDonald-Buller**

August 31, 2007

Summary

The Texas Commission on Environmental Quality sponsored a team led by the University of Texas at Austin, and including researchers at Rice University, Texas A&M University, College Station and Texas A&M University, Kingsville, to examine the concentrations of air pollutants as a function of distance from Texas roadways. Three types of roadways were examined: (1) an arterial highway, dominated by passenger vehicles (SH-71), (2) a limited access highway (freeway, I-35), and (3) a surface highway dominated by truck traffic (FM-973). This draft final report contains data on concentrations of ultrafine particles (UFPs), carbon monoxide (CO), oxides of nitrogen (NO_x), volatile organic compounds (VOCs), and several particle-bound organics and carbonyl species for the three roadways. For virtually every roadway type, and independent of whether air flow was parallel to or perpendicular to the roadway, concentrations generally decayed exponentially and returned to background levels within a few hundred meters of the roadway.

*Principal Investigator, Center for Energy and Environmental Resources, The University of Texas at Austin, 10100 Burnet Road, Bldg 133 (R7100), Austin, TX 78758, 512/475-7842, allen@che.utexas.edu

DRAFT

Background

Understanding the public health impact of roadway emissions necessitates knowledge of pollutant concentrations near roadways. Studies in Los Angeles (1) and other cities around the world (2,3) found elevated levels of pollutants near roadways which fell to background levels exponentially with increased distance from the roadway. Such data are not available in Texas, where on-road fleets and roadway design differ from previously studied locations. The Texas Commission on Environmental Quality sponsored a team led by the University of Texas at Austin, and including researchers at Rice University, Texas A&M University, College Station and Texas A&M University, Kingsville, to examine the concentrations of air pollutants as a function of distance from Texas roadways. Three types of roadways were examined: (1) a heavily traveled arterial highway, dominated by passenger vehicles, (2) a limited access highway (freeway), and (3) a heavily traveled surface highway dominated by truck traffic. This report describes the relationship between distance from roadway and concentrations for ultrafine particles (UFPs), carbon monoxide (CO), oxides of nitrogen (NO_x), Volatile Organic Compounds (VOCs) and several carbonyl species near the three roadways. In addition, maximum roadside concentrations of hydrocarbons, CO and NO_x are reported.

Sampling Locations

Samples were collected at three roadways. The first roadway sampled was Highway 71, a heavily traveled arterial highway dominated by passenger vehicles. The Hwy 71 monitoring site is shown in Figure 1 along with the site on FM-973, a heavily traveled surface highway dominated by truck traffic. The remaining roadway, I-35 north of Austin in Georgetown, is a limited access highway (freeway) and the sampling location is shown in Figure 2.

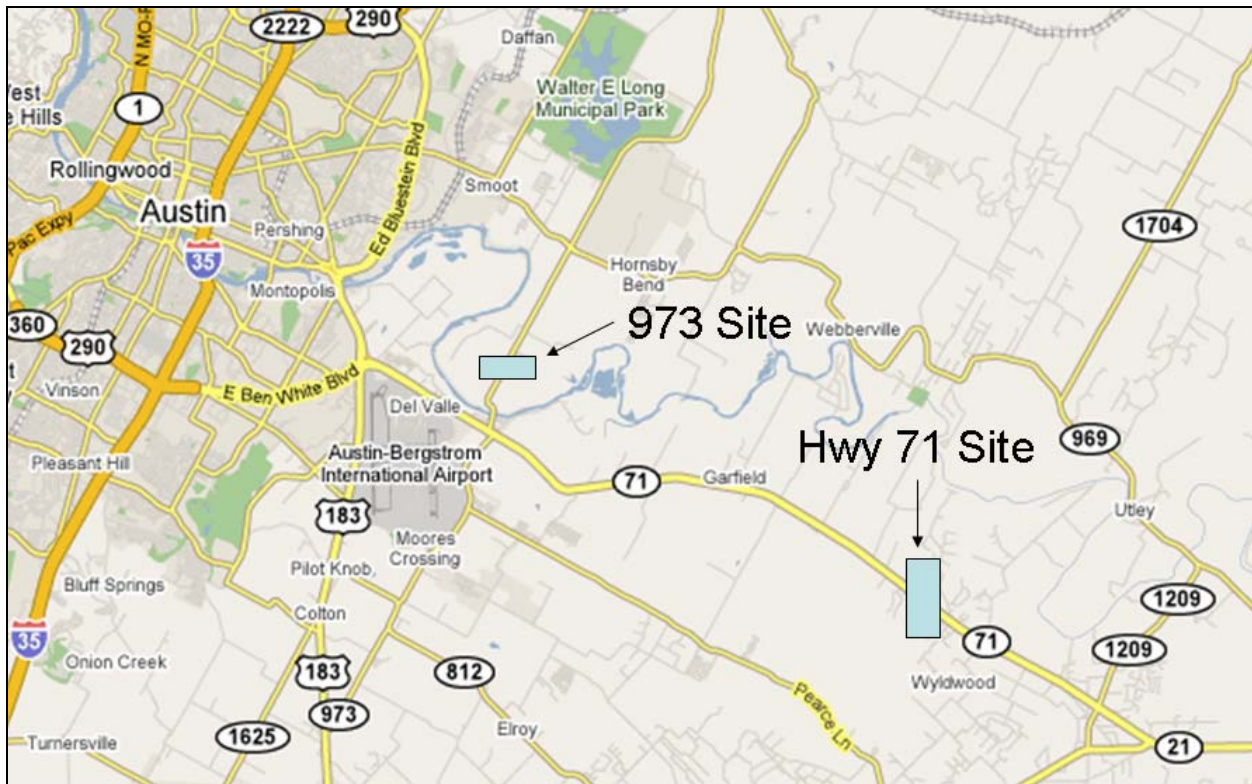


Figure 1. Sampling sites along Hwy 71 and FM-973

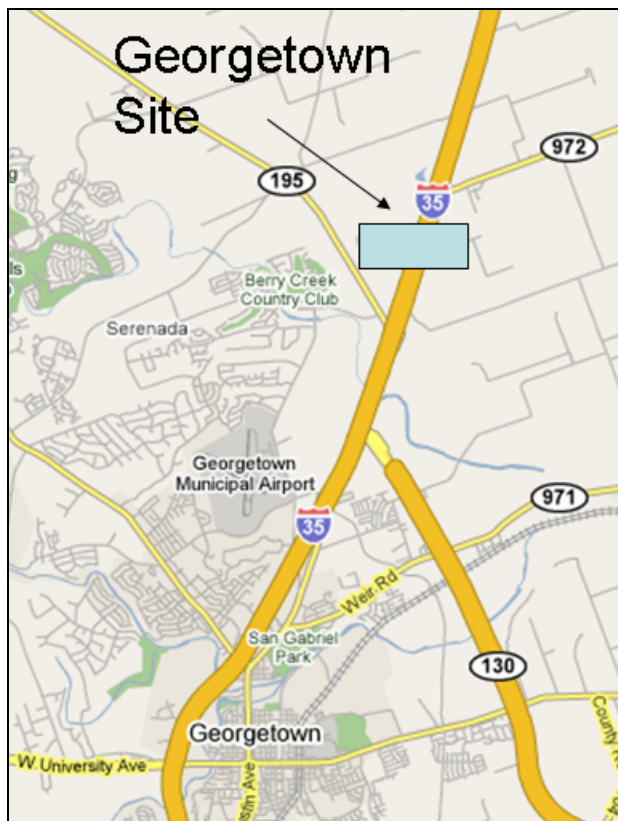


Figure 2. Sampling site on I-35

Samples were collected both upwind and downwind of each roadway. The sampling locations for Hwy 71, I-35 and FM-973 are shown with site photos in Figures 3 through 8. All roadways had an upwind stationary sampling location. Hwy 71 had two downwind stationary sampling locations, whereas I-35 and FM-973 only had one fixed downwind sample location because of limited equipment availability. The monitors at the second downwind stationary sampling trailer on the Hwy 71 site were used as the mobile sampling station on I-35 and FM-973. This mobile station was deployed at multiple downwind distances at each site. Each roadway had a mobile monitoring platform to characterize pollutant concentration falloff with increased distance from the roadway.



Figure 3. Sampling locations at the Highway 71 sampling site

The land near Hwy 71 was open and flat. Photographs taken from the site, facing upwind and downwind, are shown in Figure 4.



Figure 4. View from Hwy 71 site looking downwind (left) and upwind (right)

DRAFT

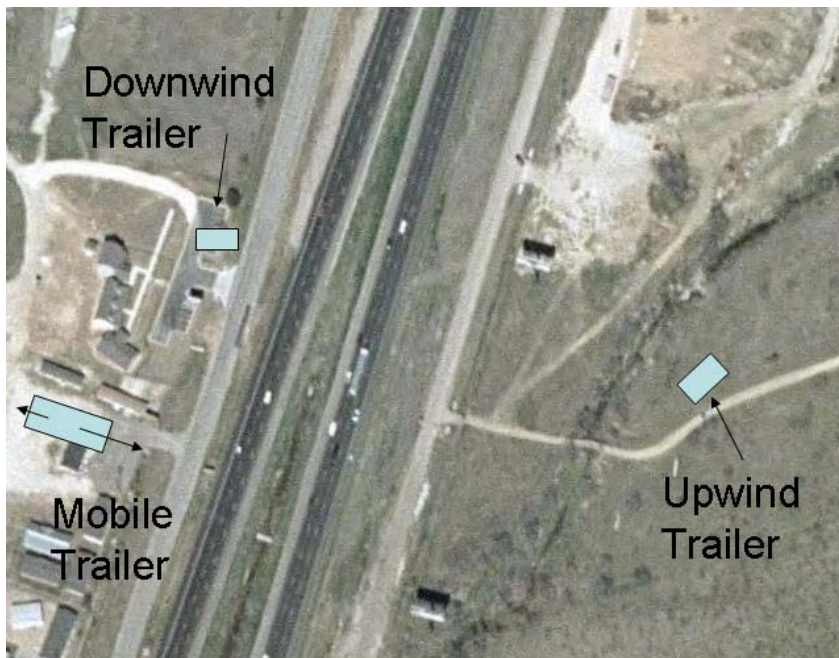


Figure 5. Sampling locations at the Interstate 35 sampling site

The land on the upwind side of I-35 was dense ground vegetation along a private unpaved driveway. The downwind side of I-35 featured a cut lawn and a small parking lot. Photographs from the site looking downwind and upwind are shown in Figure 6.



Figure 6. View from I-35 site looking downwind (left) and upwind (right)



Figure 7. Sampling locations at the FM-973 sampling site

The land along FM-973 was a lawn with several trees on the downwind side and 1-2 ft. weeds along a private driveway on the upwind side. Figure 8 shows photographs taken at the site.



Figure 8. View from FM-973 looking downwind (left) and upwind (right)

Measurements

A variety of measurements were made at the sites. Stationary trailers near Hwy 71 were located at 80 m upwind, 35 m downwind and 65 m downwind of the center of the road. On I-35 the trailers were positioned 110 m upwind and 40 m downwind. Fixed trailers for FM-973 were 80 m upwind and 15 m downwind.

DRAFT

Rice University obtained measurements of nine carbonyl species, and collected atmospheric particles on filters using low and high volume samplers. Texas A&M University at College Station measured ultrafine (less than 1 micron) particle size distributions using a condensation particle counter and a scanning mobility particle sizer at each stationary trailer. Texas A&M Kingsville (TAMUK) also used a condensation particle counter and a scanning mobility particle sizer. In addition, TAMUK utilized a mobile platform to collect data at 11 locations near Hwy 71, 9 locations near I-35, and 6 locations near FM-973.

The University of Texas measured meteorological data (wind speed and direction). Air samples were periodically collected in polished stainless steel canisters and returned to analytical laboratories at the University of Texas to determine concentrations of hydrocarbons. Video records of traffic were also collected. In the initial data collection phase (April 12 and 13), problems were encountered with the collection of CO and NO_x, so UT returned to Hwy 71 on June 11 and obtained a mobile profile of CO and NO_x concentrations during evening rush hour by sampling at a number of locations downwind of the site. During this sampling period, the CAMS site located at the airport (Austin Bergstrom KAUSE C5003) provided UT with an average wind speed and direction. Wind speeds and locations during the two periods were similar. Wind speed, wind direction, CO and NO_x were measured on Tuesday and Wednesday, July 10 and 11, 2007 near I-35 in Georgetown. Meteorological data CO and NO_x were measured near FM-973 Thursday through Saturday, July 12, 13, and 14, 2007. Three mobile samples were collected at FM-973 over this 3 day period for CO and NO_x.

DRAFT

Results and Discussion

Results are presented in the sections below. Some limited processing and analysis of the results are on-going, and will be described in supplements to this report. The measurements that have been analyzed, however, are consistent with results from previous roadway studies.

Roadway Traffic Characterization

Traffic was recorded using an 8 mm video camcorder. The camera view was angled to capture both directions of traffic flow. Later, each tape was reviewed twice, once each flow direction, to minimize the potential for counting mistakes. Vehicles were counted using a tally sheet with different categories including cars/jeeps, SUVs, vans, 4-wheel trucks, motorcycles, 6-wheel trucks 18-wheelers, dump trucks and other industrial vehicles. As continuous monitoring of traffic was not feasible due to data storage capabilities, selected samples of traffic were recorded throughout the study. The one- and two-hour samples were selected with the aim of capturing heavy traffic for each roadway. Table 1 summarizes traffic volumes and compares vehicle composition between the three roadways

Table 1. Traffic volumes (total vehicles) and percent heavy-duty vehicles

Site	Date	Times	Cars and Jeeps	Light-duty trucks	Medium-duty trucks	Heavy-duty trucks	Total Volume	#Veh /hr	% Heavy duty
Hwy 71	4/13/07	16:15 - 17:15	1238	1040	27	22	2327	2327	0.9%
I-35	7/11/07	6:40 - 8:40	1848	2321	323	727	5219	2610	13.9%
FM-973	7/13/07	7:40-9:40, 15:40-16:40	1025	1697	174	290	3186	1062	9.1%
	7/14/07	8:31 - 10:31	328	596	114	300	1338	669	22.4%

SUVs, vans and 4-wheel trucks were counted as light-duty trucks. Vehicles with two axles and six tires (i.e. four tires on the rear axle) were counted as medium-duty trucks. Heavy-duty trucks (i.e. those with three axels or more) are expected to have diesel engines. Their percentage was calculated in Table 1 for purposes of comparing to future roadways. Highway 71 is considered a low-diesel (non-industrial) highway. The traffic during the afternoon on Thursday April 13 was dominated by cars and light-duty trucks. I-35 traffic was high volume and high diesel. A weekday/weekend comparison was available for FM-973. Diesel traffic volume was the same Friday and Saturday, but the total volume was halved due to a large decrease in passenger vehicles.

DRAFT

Wind Speed/Wind Direction

Climatronics meteorological wind speed and wind direction sensors were attached to the stationary trailers and checked for direction alignment. Figure 9 shows the wind direction for Hwy 71 over the two-day period was steady from a southeasterly direction. Data was collected beginning 11 AM on April 12 and ended at noon on April 13.

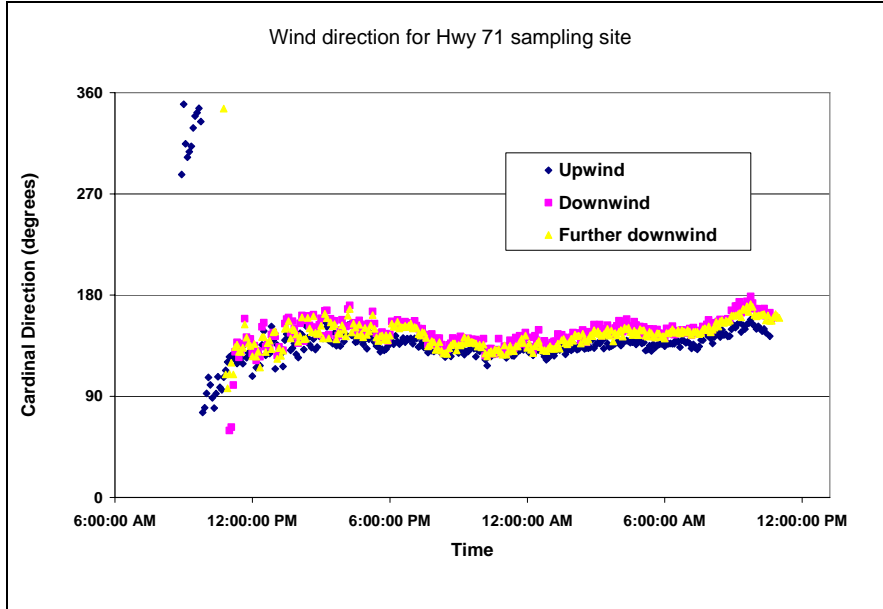


Figure 9. Wind Direction at Three Stationary Trailers near SH-71 on April 12 and 13

Figure 10 shows the wind direction on the two sides of I-35. The data, which are clustered around 180°, indicate that winds were mainly southerly. The data are consistent with observations on-site that the wind was parallel to the roadway much of the time.

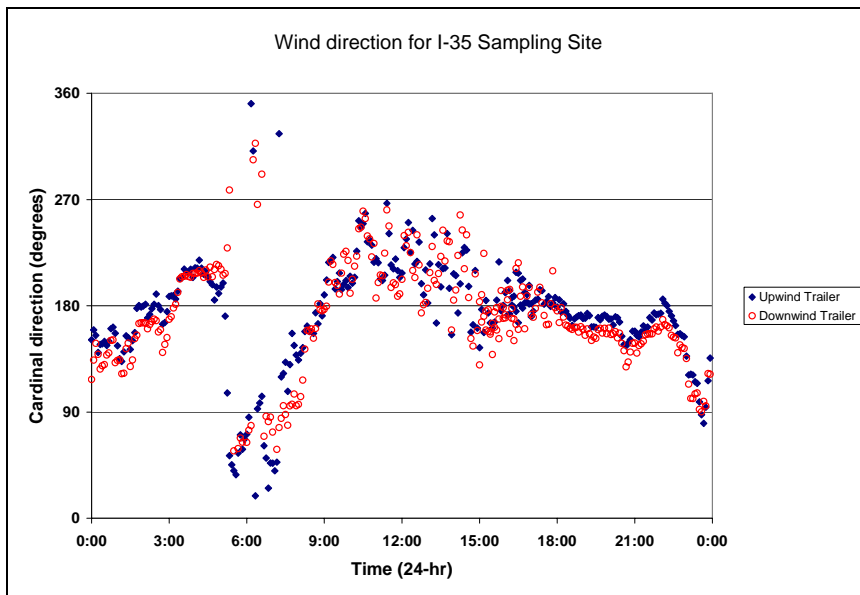


Figure 10. Wind direction at the I-35 sampling site on July 10 and 11

DRAFT

Similar to I-35, the wind direction remained largely southerly for FM-973. However as this roadway is angled Northeast/Southwest (see Figure 7), the wind was in a cross-roadway direction.

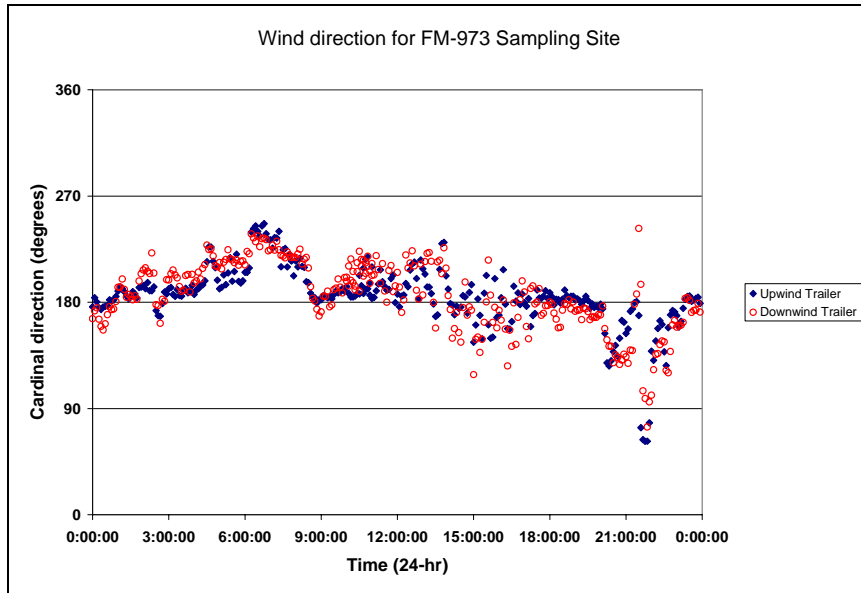


Figure 11. Wind direction for FM-973 Sampling Site on July 13 and 14

Figure 12 shows average wind speeds for the three roadways. Although they were not sampled at the same time, they are presented on the same figure for comparison. Speeds on I-35 and FM-973 were similar to one another, ranging between 2 and 8 mph. Hwy 71 averaged between 6 and 12 mph.

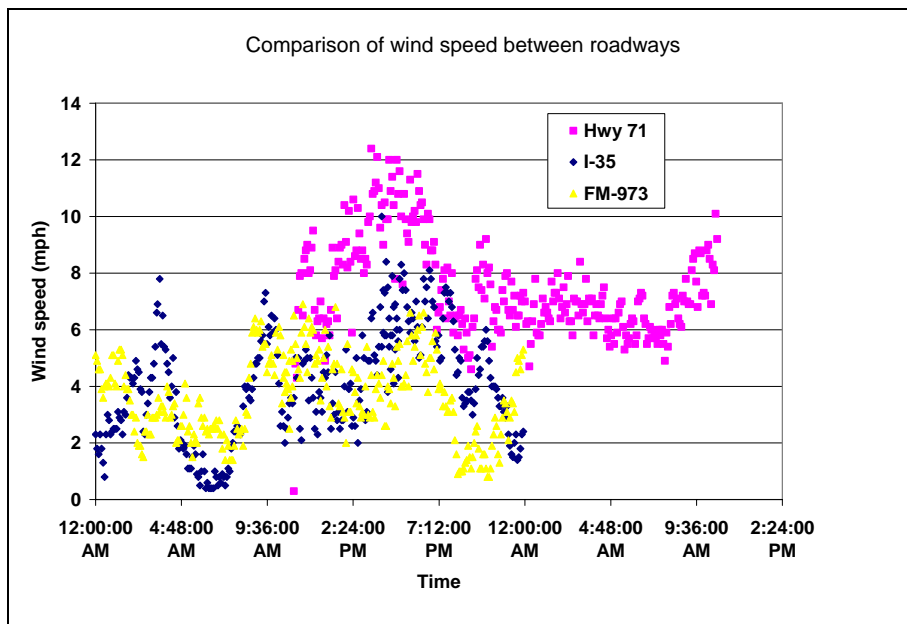


Figure 12. Wind speed comparison at the three roadway sites

DRAFT

Carbon Monoxide and Oxides of Nitrogen

Concentrations of carbon monoxide (CO), oxides of nitrogen (NO_x) and hydrocarbons were measured at the fixed trailer locations shown in Figures 3, 5 and 7. Additionally, 5 samples of CO and NO_x were measured at variable distances downwind (referred to as mobile samples) in order to capture their decay downwind of the roadways. One Hwy 71 mobile sample was collected June 11 between 4:30 and 6:45 pm. Another mobile sample was collected on July 11 between 8 and 9:30 am. The remaining three mobile samples were collected at the FM-973 site on July 12 between 2:30 and 4 pm and on July 13 during 11 am to 1 pm and 3 to 5 pm. Decay profiles were normalized by subtracting the ambient upwind concentration of the pollutant, and fitted with an exponential curve. These data are presented below.

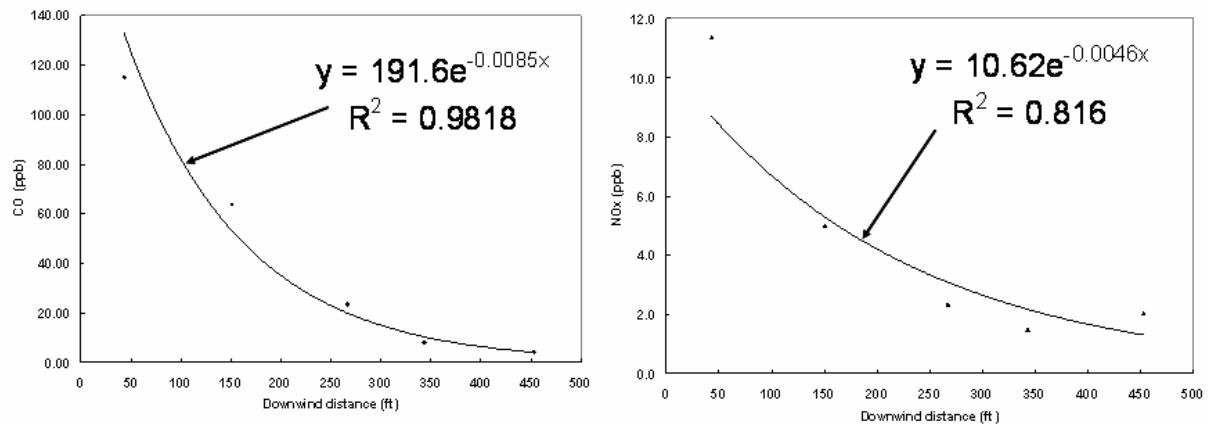


Figure 13. Normalized CO (left) and NO_x (right) measurements downwind of Hwy 71

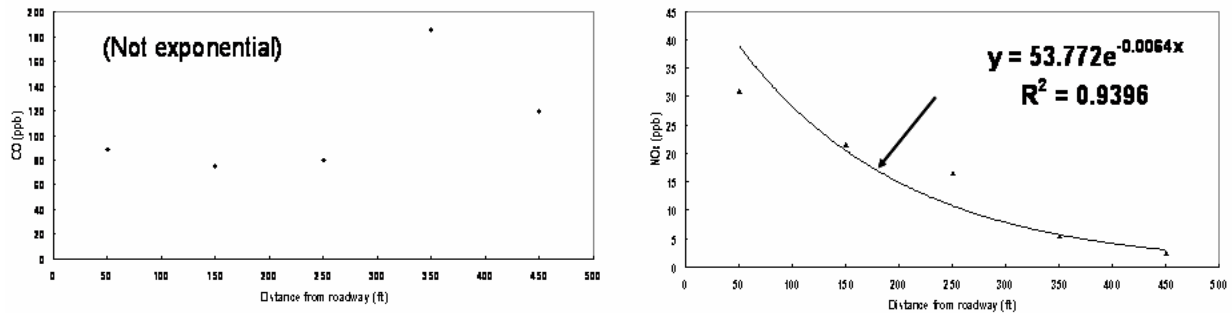
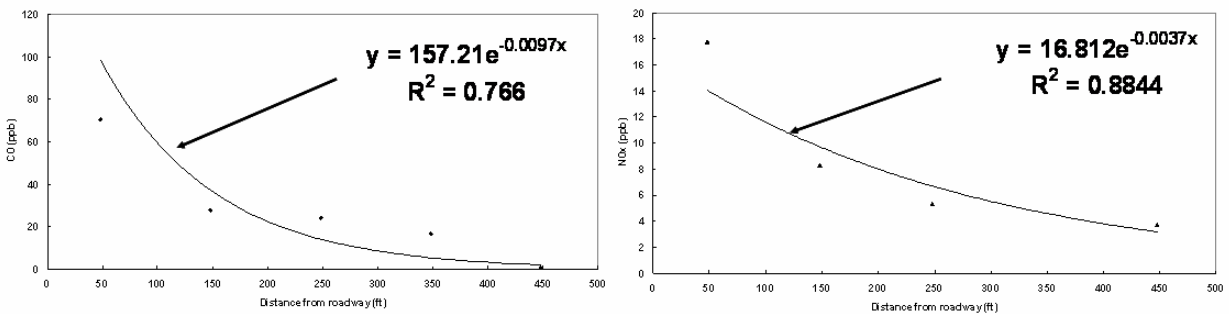


Figure 14. Normalized CO (left) and NO_x (right) measurements downwind of I-35



DRAFT

Figure 15. Normalized CO (left) and NO_x (right) measurements downwind of FM-973 (#1)

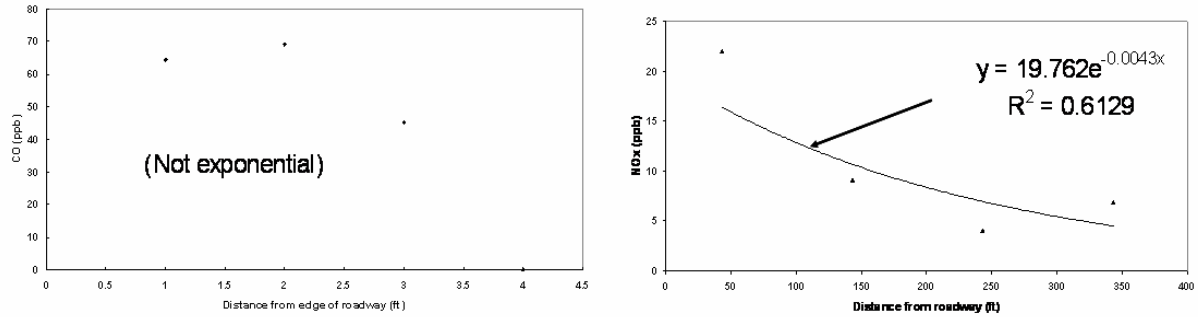


Figure 16. Normalized CO (left) and NO_x (right) measurements downwind of FM-973 (#2)

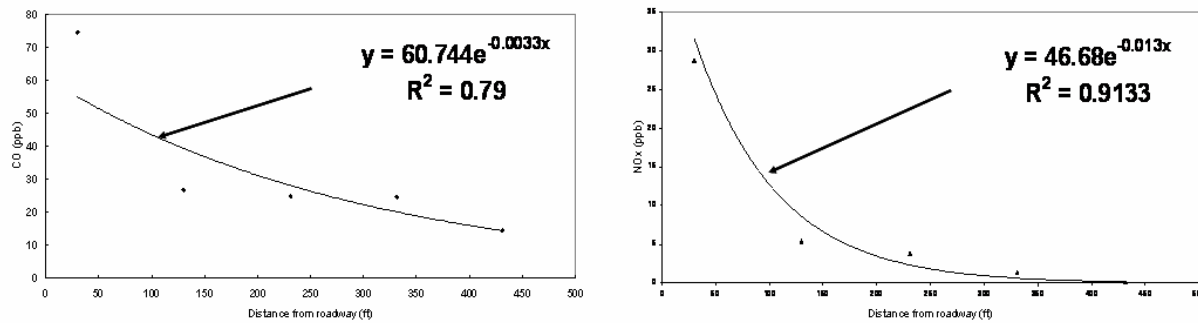


Figure 17. Normalized CO (left) and NO_x (right) measurements downwind of FM-973 (#3)

The raw data from these roadways cannot be directly compared to each other because of different wind speeds during the different sampling periods. Higher speeds produce stronger atmospheric dispersion, so the concentration profiles may not be attributable to the varying fleet characteristics of the roadways. Figure 18 represents CO concentrations normalized to a 1 mph wind speed by using the product of measured CO concentration and simultaneously measured wind speed at each sampling location.

DRAFT

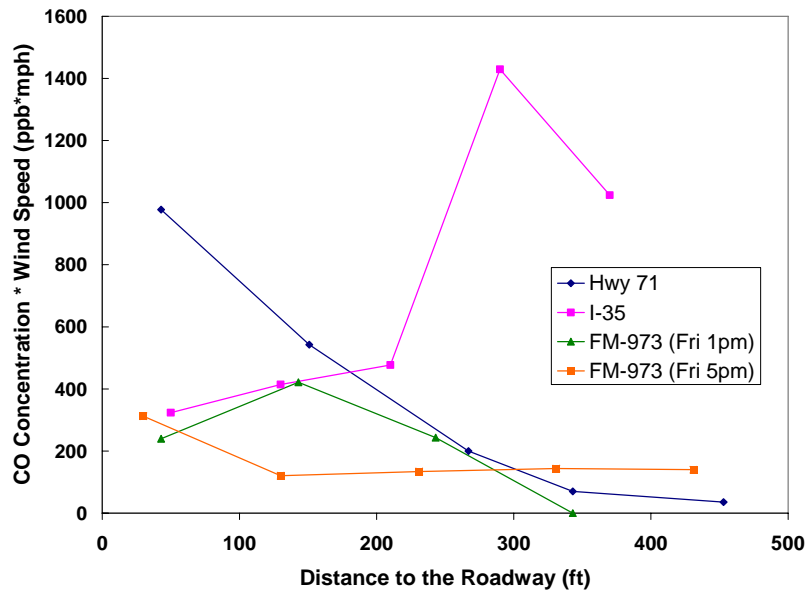


Figure 18. Measured CO concentration profiles removing effects of variable wind speed

Figure 18 shows a strong exponential decay relationship occurred only for Hwy 71. This roadway had a low percentage of diesel vehicles (1%) compared with I-35 (14%) and FM-973 (13%). The results for I-35 and FM-973 do not suggest a strong CO signature. The unusual pattern for I-35 may be due to the fact that the wind was largely parallel to the I-35 roadway during the sample period.

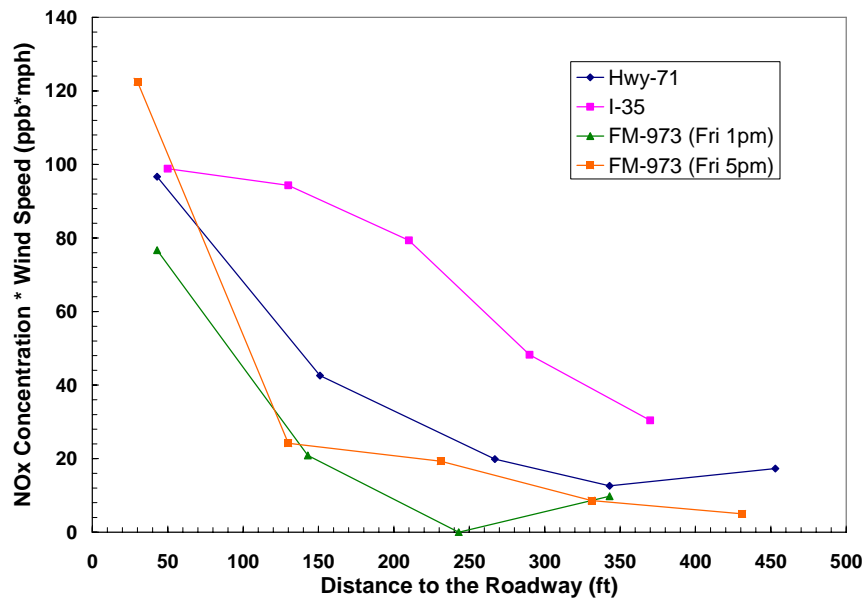


Figure 19. Measured NO_x concentration profiles removing effects of wind speed

Figure 19 reveals that the falloff of wind-normalized NO_x concentrations for SH-71 and FM-973 are similar in nature, in contrast to the profile for I-35. NO_x concentrations decrease with downwind distance from I-35, but not exponentially. This may be due to the fact that the wind

DRAFT

was largely parallel to the I-35 roadway during the sample period.

A major finding of this study is that gas phase pollutant concentrations (CO and NO_x) return to ambient levels about 400 feet (150 m) downwind of the roadway. The falloff curves vary slightly in slope, but the maximum downwind distance at which the roadway impacts local air quality is about 400 feet for all roadways studied.

Maximum concentrations of pollutants observed near roadways are relevant for exposure assessment. Table 2 below lists the maximum 5-minute average concentrations of CO and NO_x measured at the stationary trailers downwind of I-35 and FM-973, respectively. The times of day when the maxima occurred are noted in parentheses.

Table 2. Maximum Roadside Concentrations of Pollutants

Roadway	CO (ppb)	NO _x (ppb)
I-35	415 (7:35 AM)	102 (5:40 AM)
FM-973	562 (4:30 PM)	102 (6:50 AM)

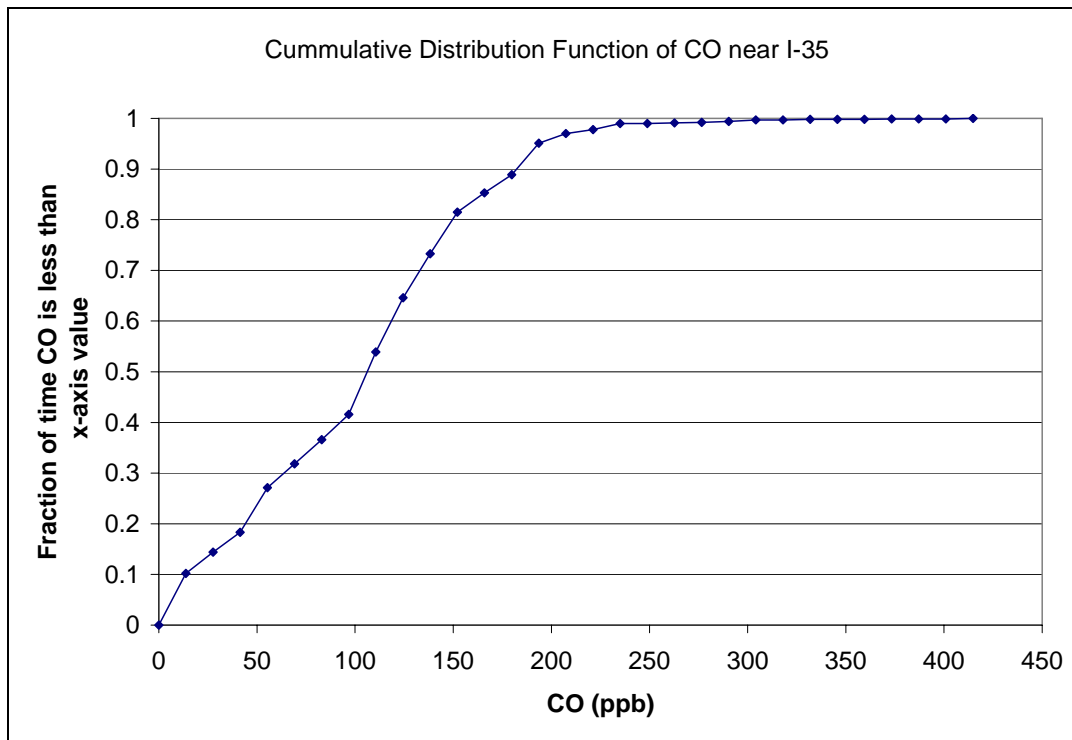


Figure 20. Distribution function of roadside CO concentrations for I-35

DRAFT

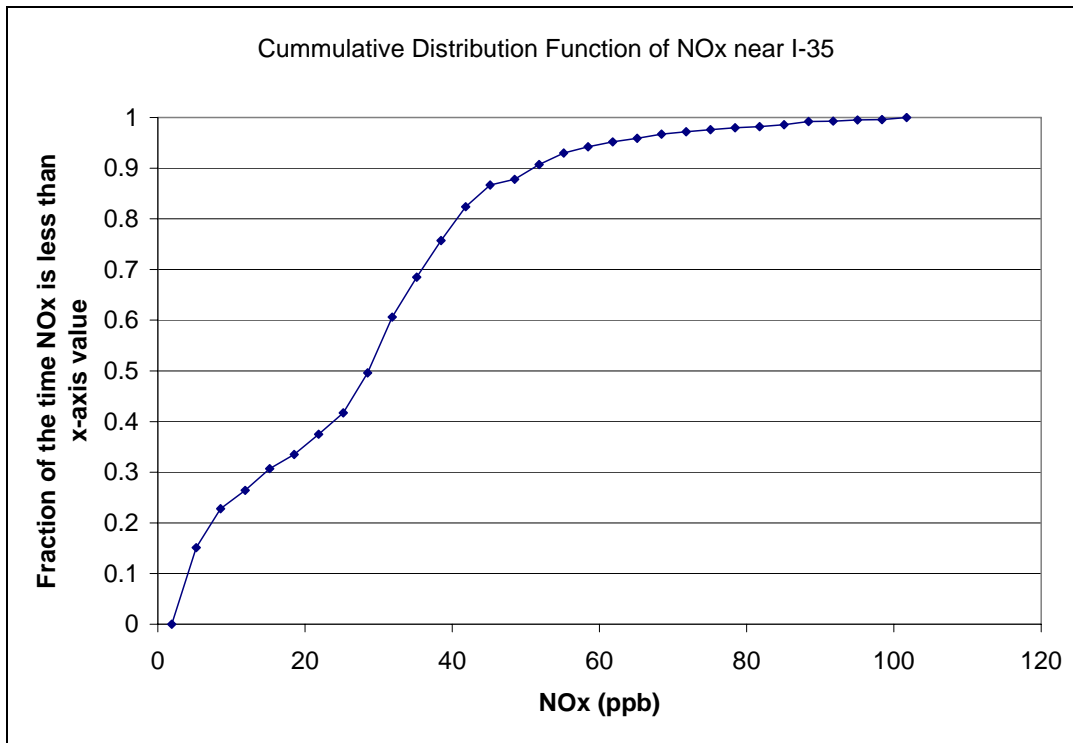


Figure 21. Distribution function of roadside NOx concentrations for I-35

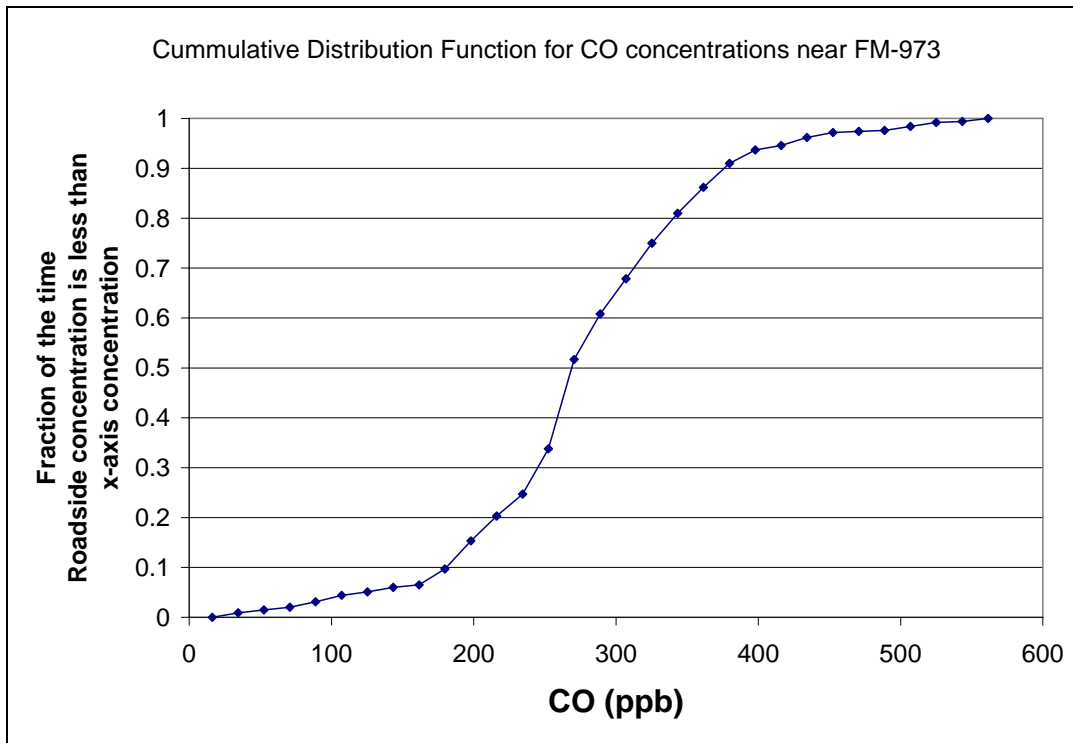


Figure 22. Distribution function of roadside CO concentrations for FM-973

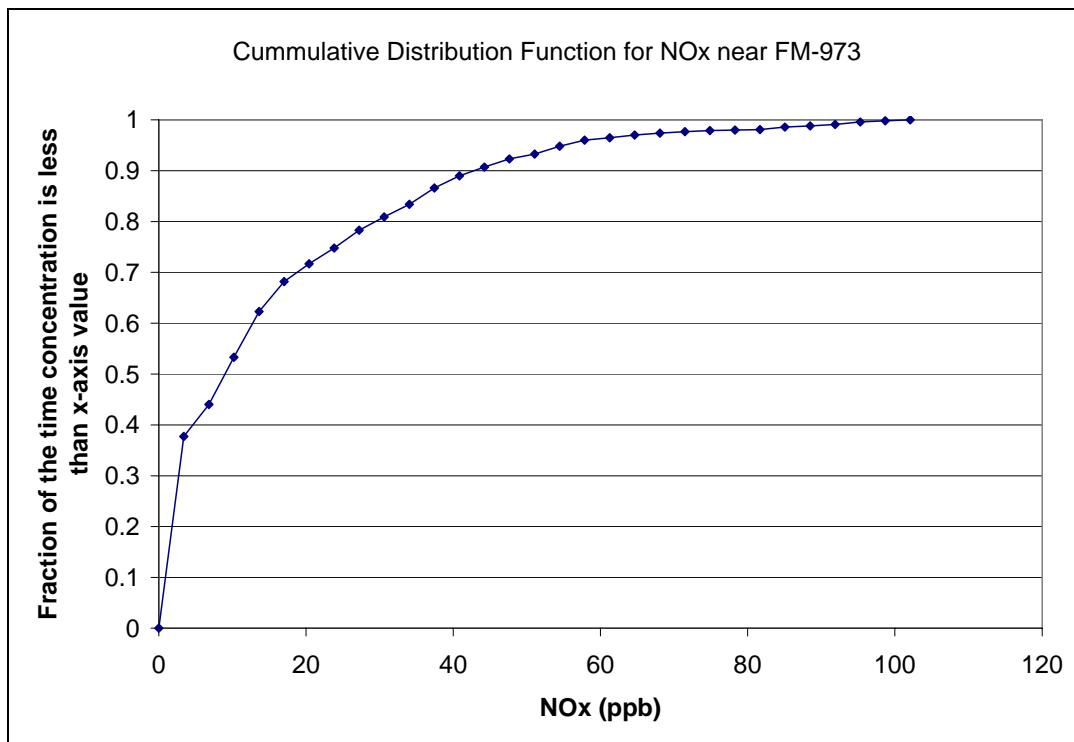


Figure 23. Distribution function of roadside NOx concentrations for FM-973

DRAFT

Ultrafine Particle Concentrations

Figure 24 shows the sampling locations of the two fixed trailers and the mobile platform near the SH-71, I-35 and FM-973 roadways. Blue rectangles indicate stationary trailers. Red stars indicate mobile platform sampling points. Distances from each sampling point to the middle of the roadway were also given in the figure.

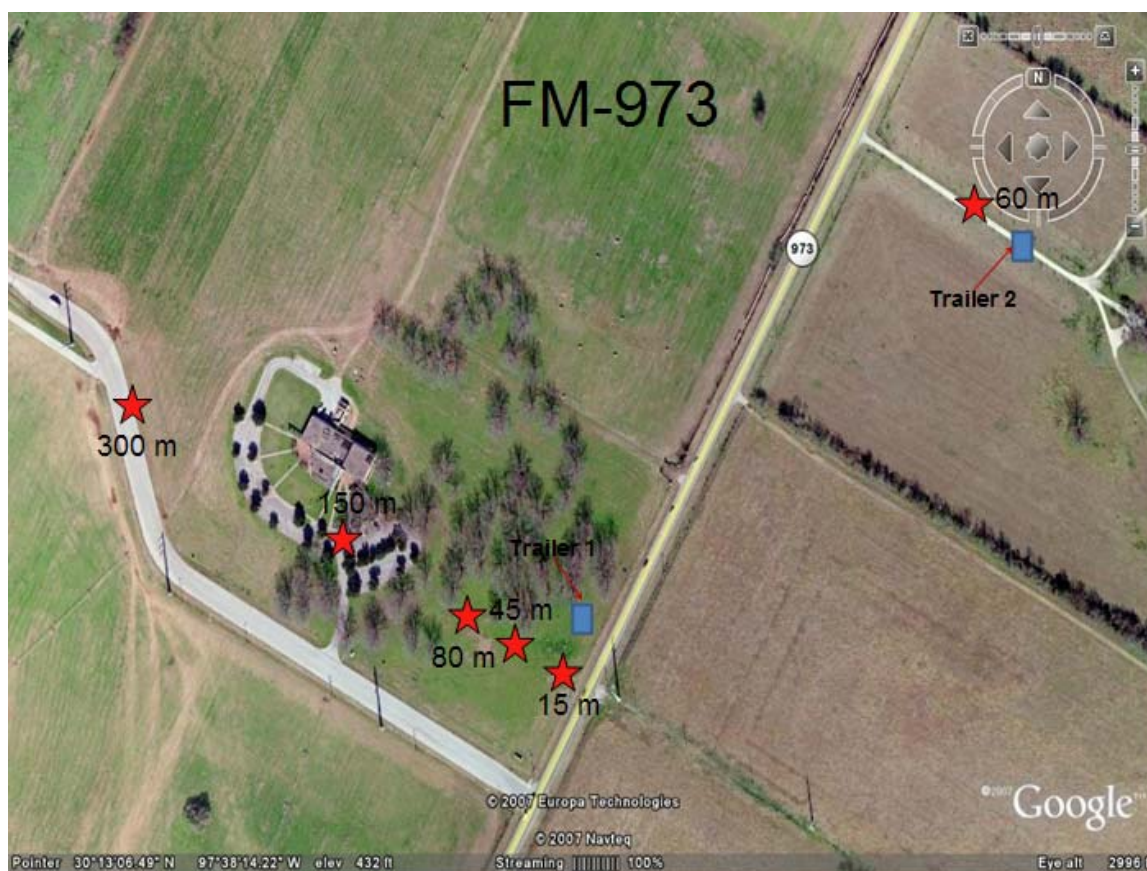


(a) SH-71

DRAFT



(b) I-35



(c) FM-973

Figure 24. Sampling locations near (a) SH-71, (b) I-35, and (c) FM-973 sampling site. Blue rectangles indicate stationary trailers. Red stars indicate mobile platform sampling points.

Table 3 summarizes measured traffic volume, wind speed, and particle number concentrations at the closest mobile downwind site of the three Texas roadways. Data from a previous study, collected by Zhu et al. (1), at 30 m downwind of the I-405 freeway in Los Angeles during summer daytime are included for comparison. Ratios of particle number concentrations near these roadways are also included in Table 3b. Standard deviations are included in parentheses. The particle number concentration near I-405 (LA) was about 7.5 times of that measured near the SH-71. This ratio is very close to the total traffic volume ratio (7.3) observed for the two roadways.

Although total traffic volume on the SH-71 was 1.8 times the volume on FM-973, the observed particle number concentrations were similar near the two roadways. Three factors may explain this apparent discrepancy. First, although the total traffic volume on the FM-973 was lower, the number of diesel trucks was higher than SH-71. Since diesel vehicles emit much higher concentrations of ultrafine particles than gasoline cars, higher diesel traffic will likely contribute to the observed higher particle number concentrations near the FM-973. Second, wind speeds were lower during the FM-973 sampling period. Lower wind speeds result in weaker atmospheric dispersion which leads to higher ultrafine particle number concentrations. Finally, the nearest sampling location near FM-973 was closer to the highway (15 m) compared to other

DRAFT

roadways. It has been shown that particle number concentrations decay exponentially at increasing distances downwind of roadways. Since the nearest sampling location is at the steepest part of the exponential decay curve, a few meters closer to the roadway will likely result in higher pollutant concentrations. This also helps explain the relatively low particle number concentrations measured at the closest sampling point to I-35 (40 m from the middle of the roadway).

Table 3. Comparison of (a) values and (b) ratios between measured traffic volume, wind speed, and particle number concentrations near Texas and Los Angeles Roadways.

(a)

	SH-71	I-35	FM-973	I-405
Distance from the road	20	40	15	30
Total Vehicle [# min ⁻¹ , (s.d.)]	31.85 (9.15)	76.02 (18.16)	17.34 (4.24)	231.24 (129.88)
Diesel Trucks [# min ⁻¹ , (s.d.)]	1.58 (0.89)	14.12 (4.20)	5.91 (2.16)	9.29 (4.53)
Gasoline Cars [# min ⁻¹ , (s.d.)]	28.45 (7.98)	61.89 (15.41)	11.44 (3.81)	221.95 (28.77)
Wind Speed [m s ⁻¹ , (s.d.)]	3.3 (0.9)	2.0 (0.9)	2.0 (0.6)	1.5 (0.6)
Particle Number Concentration [cm ⁻³ ,(s.d.)]	2.0e4 (1.0e4)	1.4e4 (0.7e4)	2.0e4 (1.6e4)	1.5e5 (3.1e4)

(b)

	I-405/ SH-71	I-405/ I-35	I-405/ FM-973	SH-71/ I-35	SH-71/ FM973	I-35/ FM973
Total Vehicle (# min ⁻¹)	7.3	3.0	13.3	0.4	1.8	4.4
Diesel Trucks (# min ⁻¹)	5.9	0.7	1.6	0.1	0.3	2.4
Gasoline Cars (# min ⁻¹)	7.8	3.6	19.4	0.5	2.5	5.4
Wind Speed (m s ⁻¹)	0.5	0.8	0.8	1.7	1.7	1
Particle Number Concentration (cm ⁻³)	7.5	10.7	7.5	1.4	1	0.7

Figure 25 shows measured and predicted Ultrafine Particle (UFP) number concentration decay profile near SH-71. Data were normalized to 1 m s⁻¹ wind speed by using the product of measured particle number concentrations and simultaneously measured wind speed at each sampling location. Dark circles represent mean particle number concentrations measured at different distances from the roadway. Error bars represent one standard deviation of measured particle number concentrations. Open circles represent predicted particle number concentrations based on the fitted exponential decay function using measured data.

DRAFT

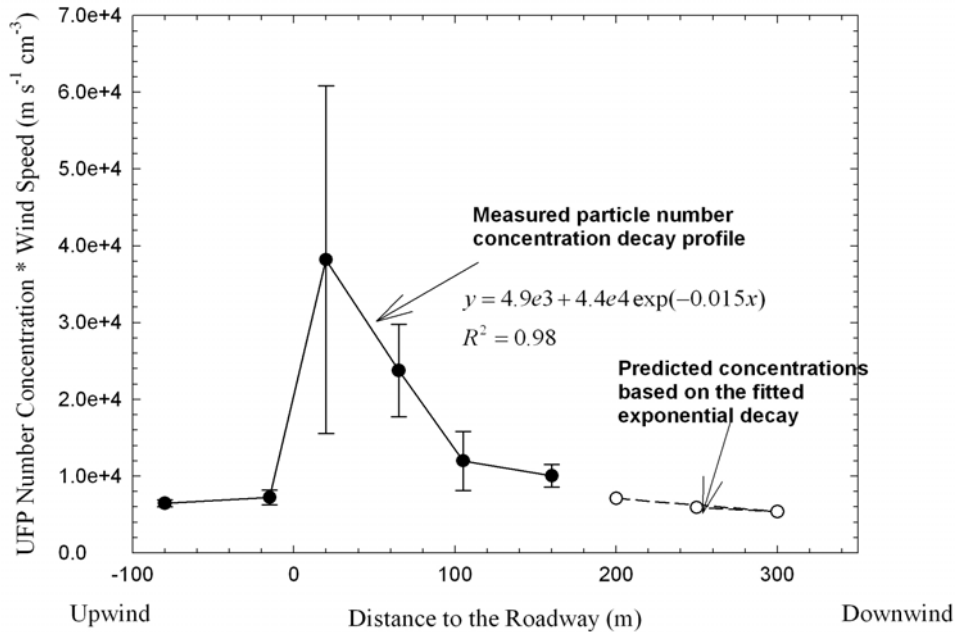


Figure 25. Measured and predicted UFP number concentration decay profile near SH-71

Data collected beyond 160 m on the downwind side of the roadway were not included in the graph because wind directions were too close to being parallel to the roadway during those measurements. Similar to what reported previously near the Los Angeles Freeways, particle number concentrations increased dramatically moving from the upwind side to the downwind side of the roadway. The elevated particle number concentrations decays exponentially with increasing distances from the roadway. Particle number concentrations dropped sharply within the first 100 m and were comparable to what was measured upwind of the roadway at 200-300 m downwind of the roadway. No significant concentration gradient was observed for particle number concentrations on the upwind side of the SH-71. All of these are in agreement with previous Los Angeles freeway studies.

The wind direction was generally parallel to I-35 on July 10th and 11th. Occasionally, the wind was across the roadway from the east on the 10th and west on the 11th. Figure 26 shows the spatial profile for total particle number concentration near the I-35 freeway under these crosswind conditions. The dominant wind directions on both sampling days are also shown in the figure. No significant concentration gradient was observed for particle number concentrations on the western (upwind) side of the I-35 freeway on July 11th (Figure 26b). The exponential decay profile occurred on the downwind side of the roadway. Thus, when wind direction switched from July 10th to 11th, the fall-off decay curve occurred on the different side of the I-35. This is in agreement with previous Los Angeles freeway study in which ultrafine particle decay curves were observed on the other side of the I-405 freeway when the wind switched direction at night (4).

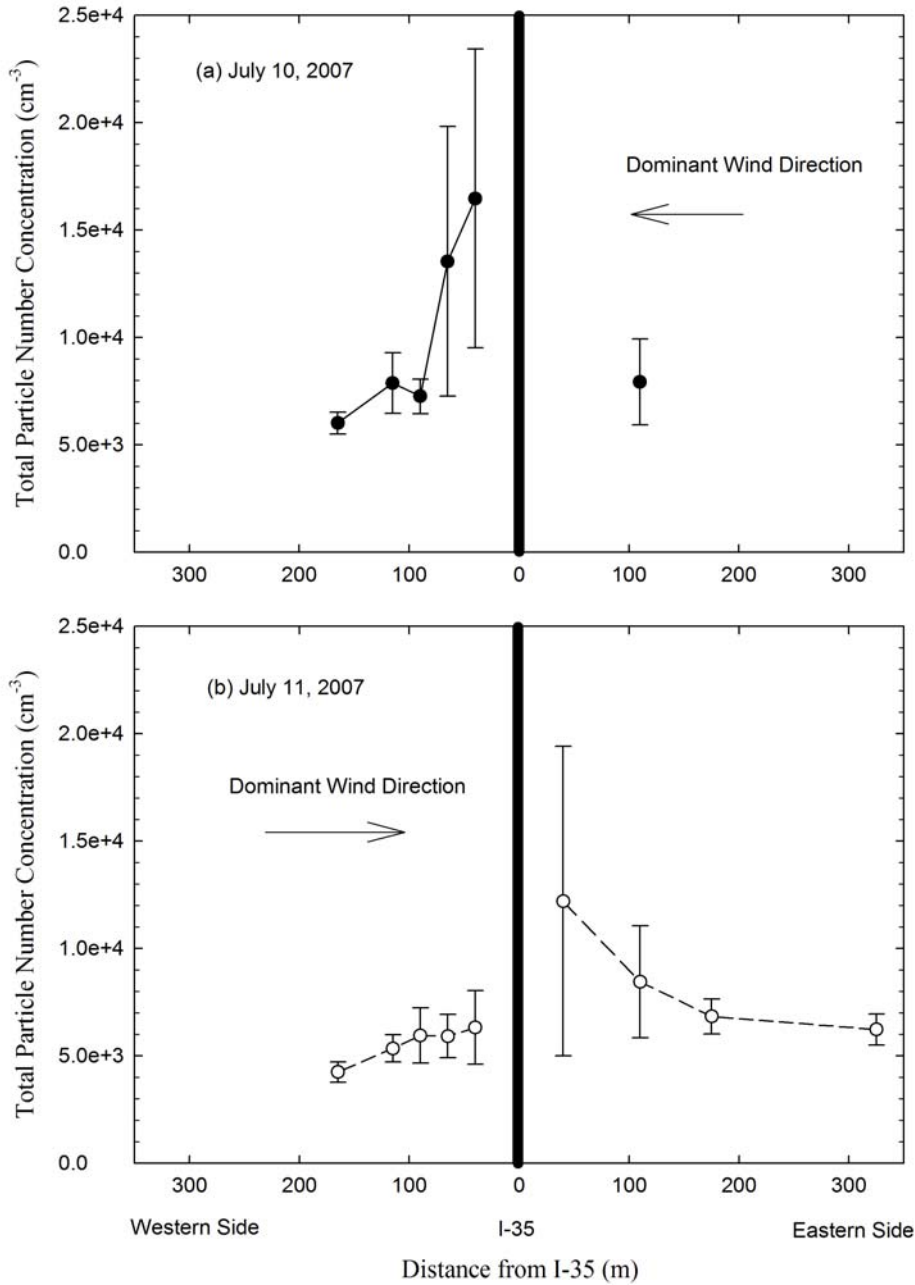


Figure 26. Measured ultrafine particle number concentration decay profile near I-35.

Figure 27 shows the spatial profile for total particle number concentration near the FM-973 measured by the CPC on July 12th, 13th, and 14th. The wind directions on all sampling days were consistent and particle number concentration gradient was observed on the same side of the FM-973 for all three days.

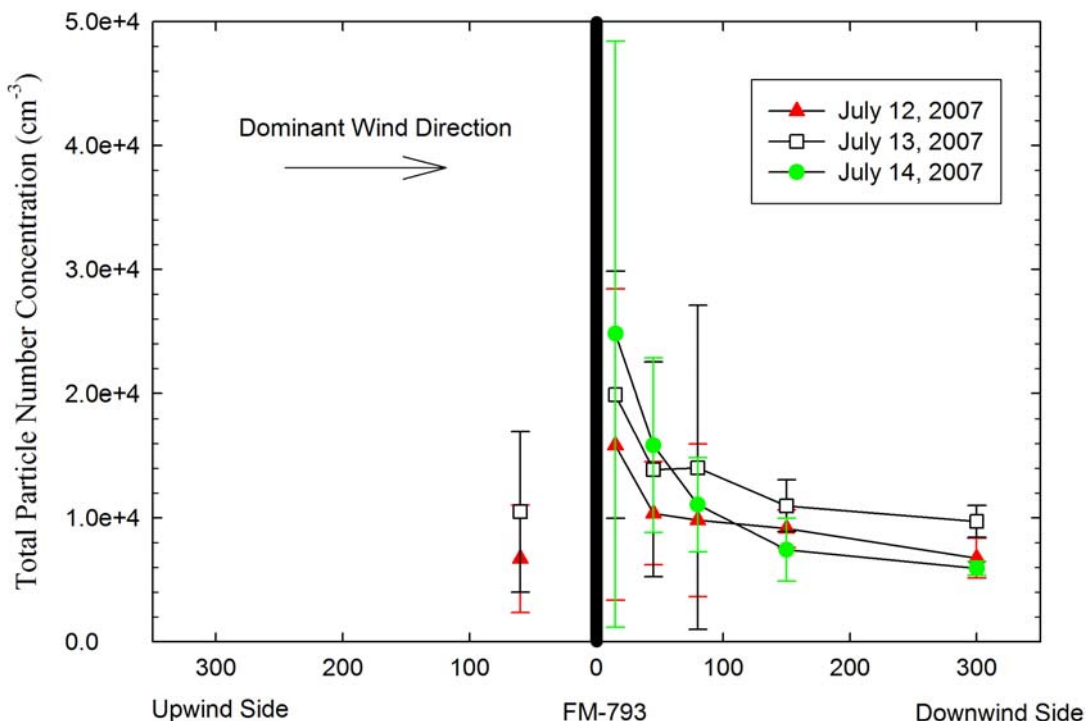


Figure 27. Measured ultrafine particle number concentration decay profile near FM-973.

As shown in Figures 25-27, for all three roadways, particle number concentration decreased about 60% in the first 100 m and then leveled off somewhat after 150 m, similar to what Zhu et al., (1) reported for Los Angeles freeways. Exponential decay curves were used for ultrafine particle dispersion near the Los Angeles freeways. Similar exponential decay characteristics were observed for all three Texas roadways. Ultrafine particle concentrations observed 300 m downwind of the Texas roadways were similar to background (upwind) concentrations. Again, this is in agreement with previous Los Angeles studies, and with measurements of gas phase pollutants near Texas roadways.

Figure 28 shows typical observed ultrafine size distributions from vehicular emissions near SH-71, I-35 and FM-973 when diesel trucks were present, and in the background air. It is well known that ultrafine from vehicular exhaust usually exhibit a bi-modal size distribution with a primary mode between 10 and 30 nm and a secondary mode between 50 and 70 nm (5-7). This is also true in the current study especially when diesel trucks were present on roadways. The primary mode (10-30 nm) only exists in significant amounts on or near freeways (1;8-10) such as observed in the current study. Ultrafine particle concentrations observed at downwind sites near the roadways were much higher than background levels. No primary mode was observed for the background air which was also in excellent agreement with previous studies.

DRAFT

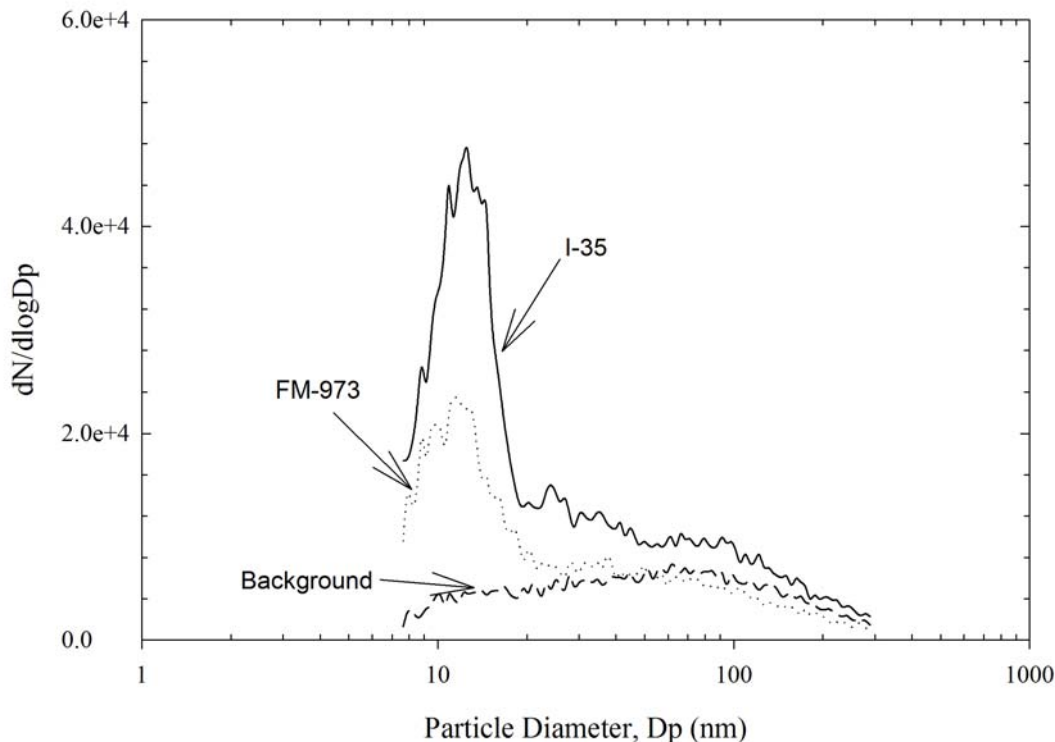


Figure 28. Typical ultrafine particle size distributions near the SH-71, I-35 and FM-973 roadways when diesel trucks were presented and at the background site.

Particle size distributions were also measured in fixed locations. Typical results for these measurements are shown in Figure 29. The vertical axis in the color plots in Figure 29 is the particle size; the horizontal axis is time, and the colors give an indication of particle number concentration. The uppermost panel indicates that in general, if times with high background concentrations are discounted, the concentrations of UFPs exhibited the following order: near downwind > far downwind > upwind. Bimodal size distributions with peaks at 10 nm and 100 nm were observed. Figure 30 shows the average size distributions observed during the two periods shaded in Figure 29 (upper is earlier time period, lower is later time period). Figures 31 and 32 show the same type of data for a different time period.

DRAFT

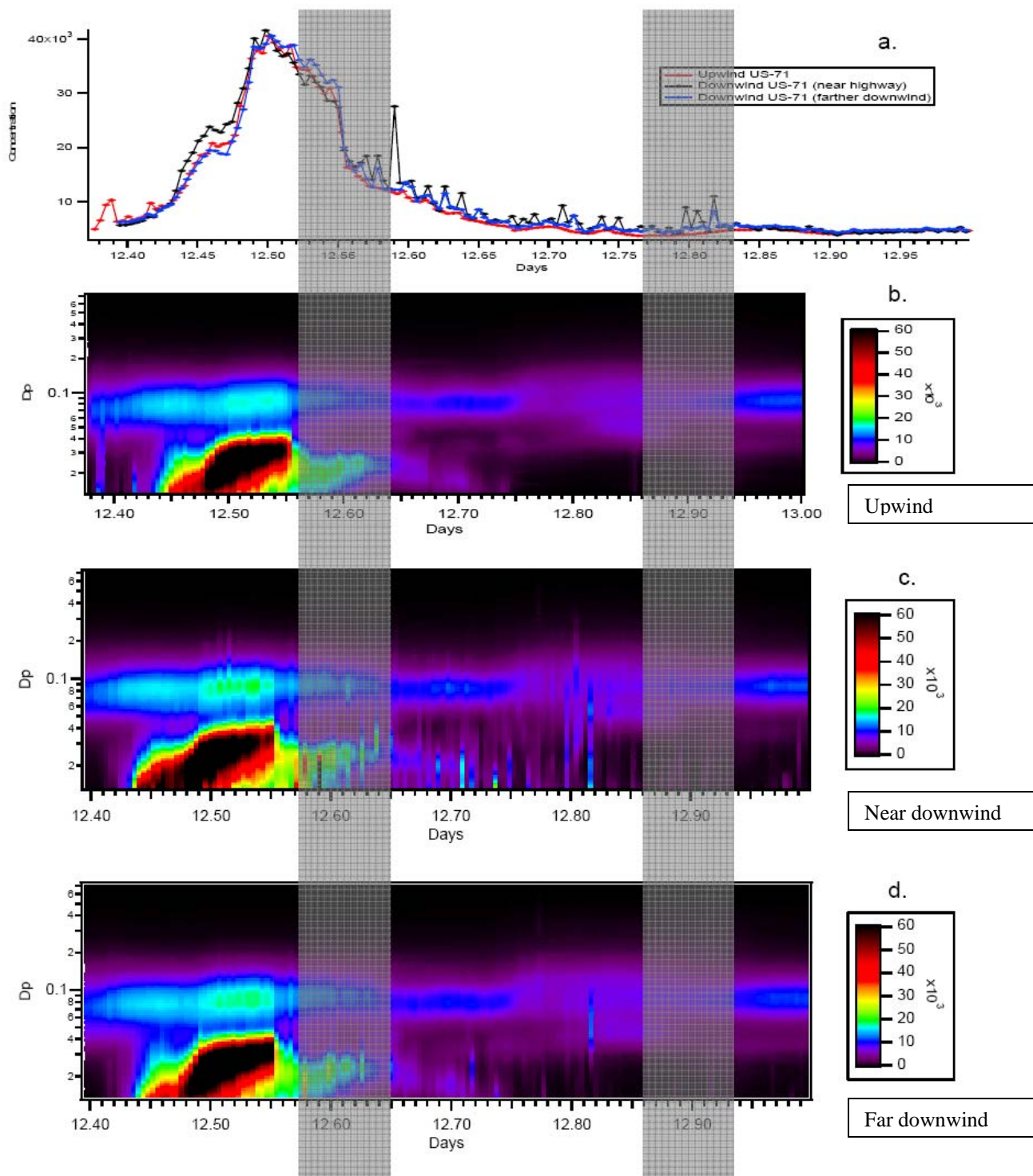


Figure 29. Particle number and size distributions measured at fixed sites near highway 71; the vertical axis in the color plots is the particle size; the horizontal axis is time, and the colors give an indication of particle number concentration. The uppermost panel indicates that in general, if times with high background concentrations are discounted, the concentrations of UFPs exhibited the following order: near downwind>far downwind>upwind. Bimodal size distributions with peaks at 10 nm and 100 nm were observed.

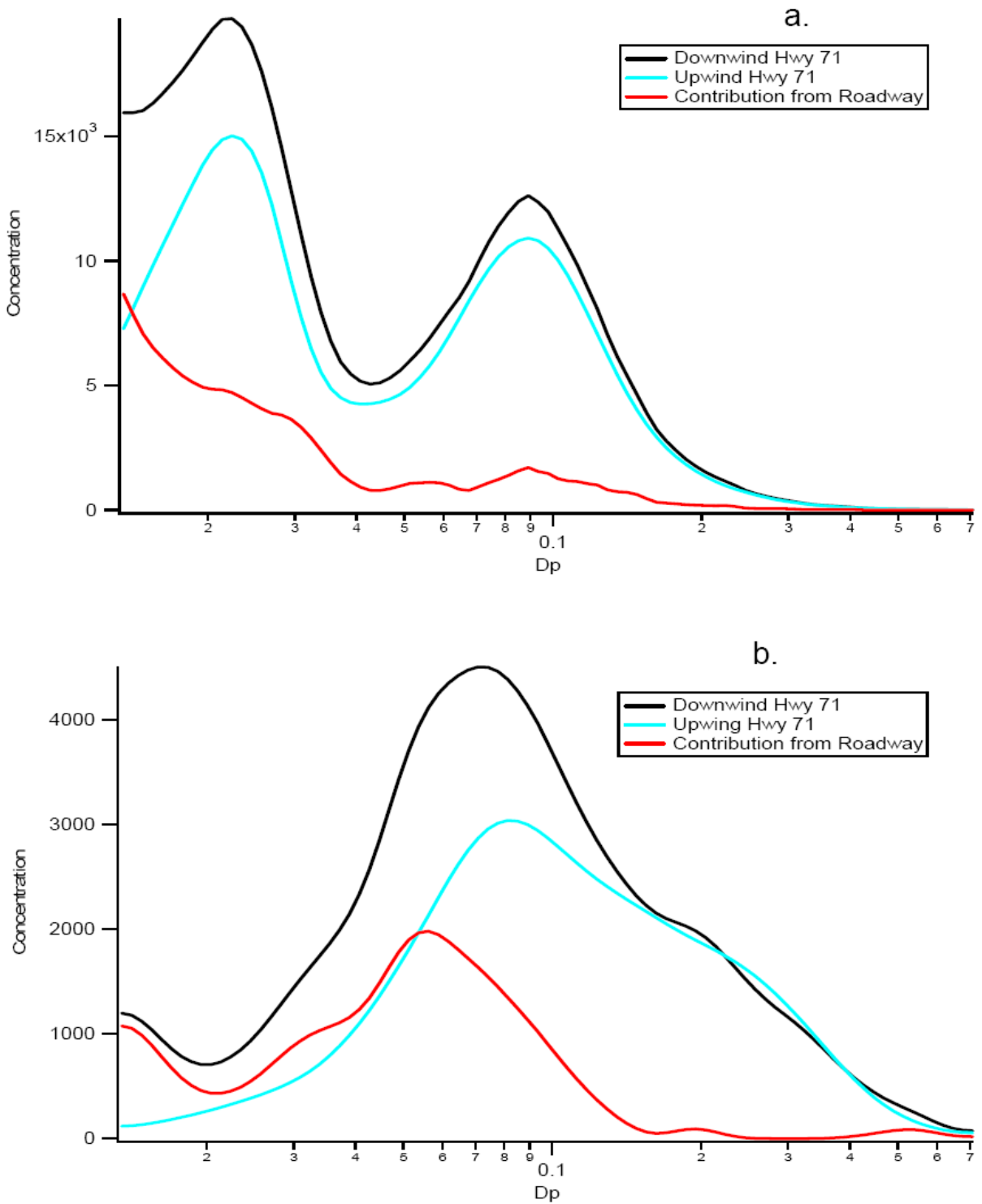


Figure 30. Average size distributions observed during the two periods shaded in Figure 29 (upper is earlier time period, lower is later time period)

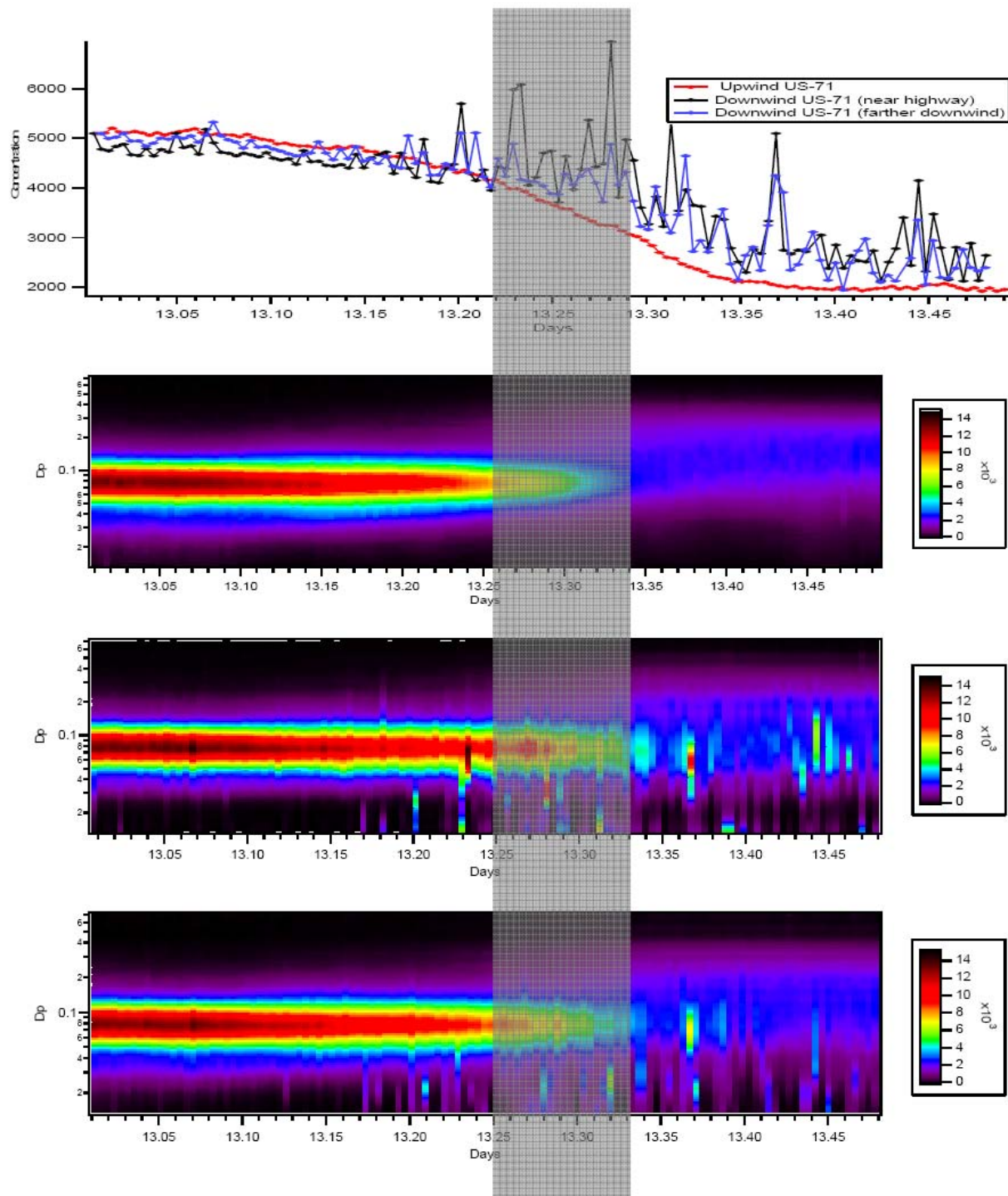


Figure 31. Particle number and size distributions measured at fixed sites near highway 71; the vertical axis in the color plots is the particle size; the horizontal axis is time, and the colors give an indication of particle number concentration. The uppermost panel indicates that in general, if times with high background concentrations are discounted, the concentrations of UFPs exhibited the following order: near downwind>far downwind>upwind. Bimodal size distributions with peaks at 10 nm and 100 nm were observed

DRAFT

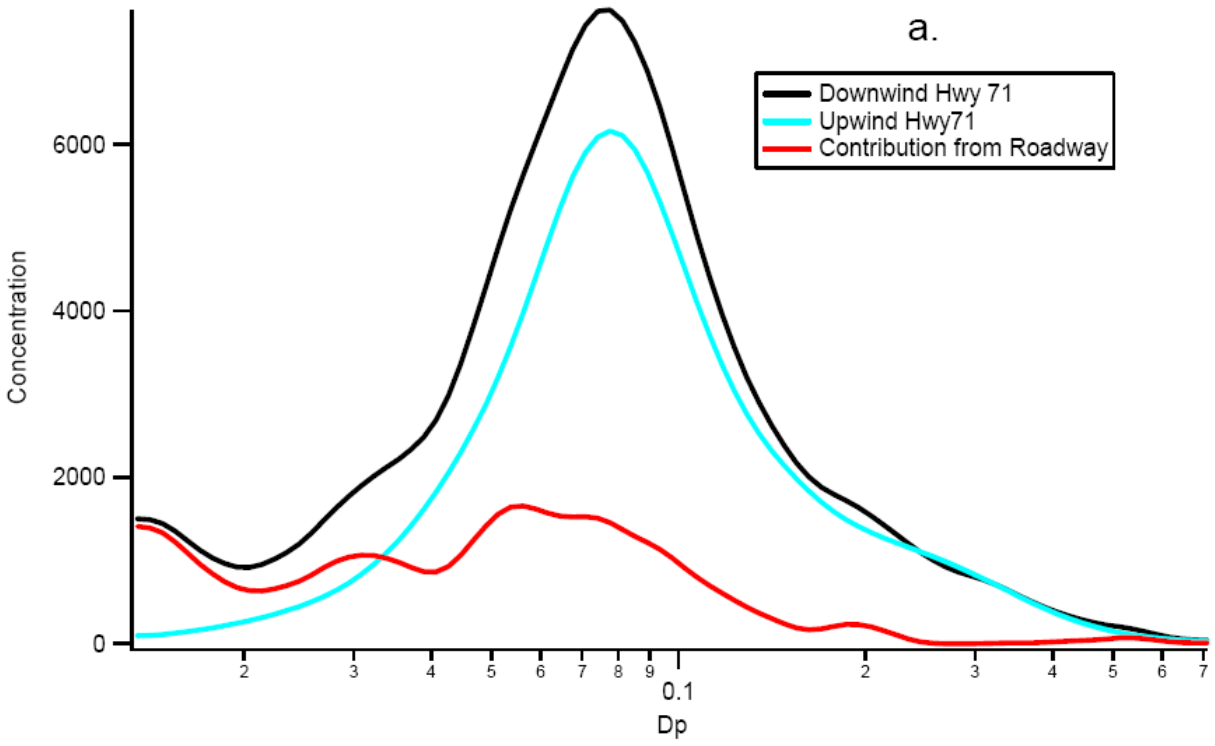


Figure 32. Average size distributions observed during the period shaded in Figure 31.

DRAFT

An Unexpected Nucleation Event

On April 12, 2007 from about 11:10 AM to 12:10 PM, we observed an unexpected nucleation event on the upwind side of the roadway as shown in Figure 33a. For comparison, a typical time series of particle number concentration collected at 20 m downwind of the SH-71 is presented in Figure 33b.

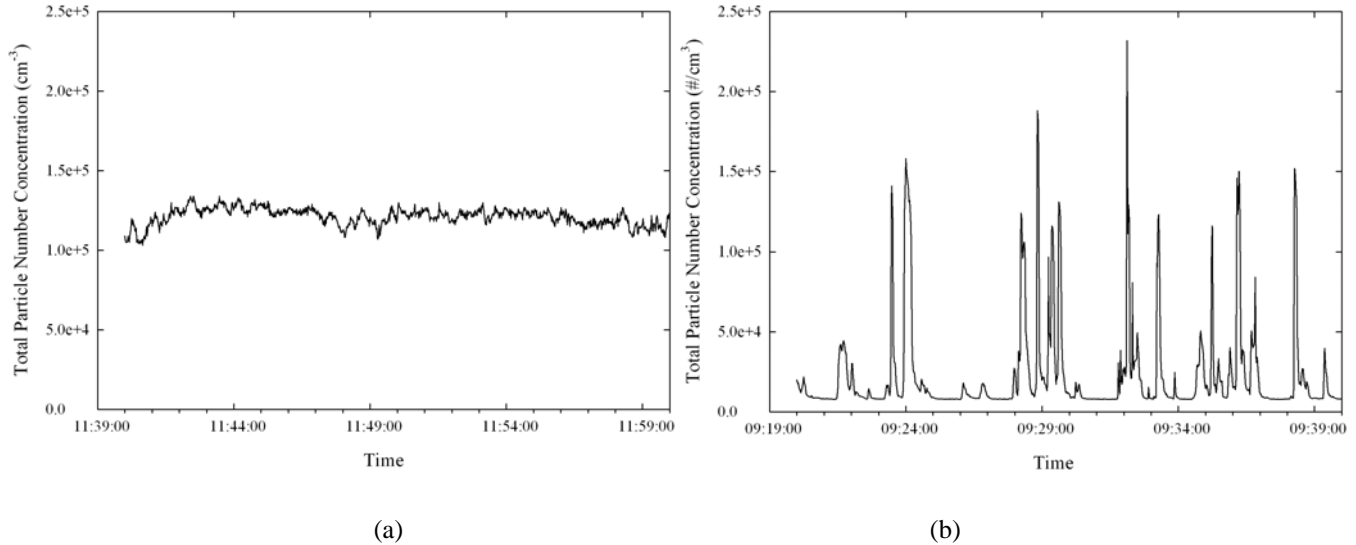


Figure 33. Typical time series of observed particle number concentrations (a) during a nucleation event and (b) from roadway traffic emissions on April 12, 2007.

Identical concentration scales for the y-axis are used for both figures. It is seen that UFPs from traffic emissions were characterized by individual peaks on a time-series plot that corresponding to individual passing vehicles (Figure 33b). On the other hand, the nucleation event period was characterized by uniformly distributed higher particle number concentrations on the upwind side of the roadway as shown in Figure 33a. It is noted, the time series plot presented in Figure 33a were collected at several upwind locations with increase distances from the roadway. No spatial profile was observed due to a uniformly distributed regional nucleation event.

DRAFT

PM_{2.5} Mass Concentrations and Ions

Low-volume quartz fiber filters were located at 80 m upwind, 35 m downwind and 65 m downwind of the center of SH-71; 110 m upwind and 40 m downwind of I-35, and 80 m upwind and 15 m downwind of FM-973. Sampling dates and times are provided in Appendix A. Ambient fine particulate mass concentrations were determined as well as chloride, nitrate, nitrite, sulfate, sodium, magnesium, calcium, potassium, and ammonium. Note that upwind concentrations were plotted at 0 m downwind for clarity.

Figure 34 shows the falloff of PM_{2.5} mass concentrations from the vicinity of the three roadways. The PM_{2.5} profile illustrates classic falloff behavior with low concentrations upwind of the roadway, the greatest concentration immediately downwind of the source, decreasing concentrations further downwind from the roadway. Figures 35 through 37 show the falloff of ions near SH-71, I-35, and FM-973, respectively. Concentrations of ions near SH-71 and FM-973 exhibit falloff behavior similar to that of PM_{2.5} mass concentrations; in contrast ion concentrations show relatively little difference upwind and downwind of I-35, likely due to the wind direction being parallel to the road.

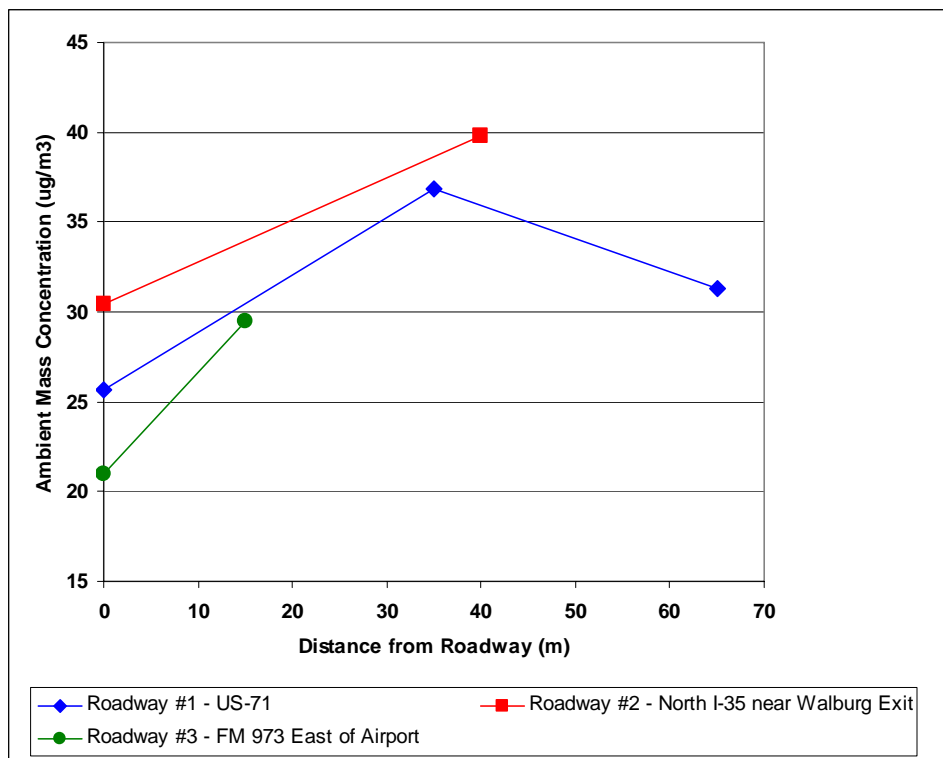


Figure 34. Roadway falloff of PM_{2.5} mass concentrations near SH-71, I-35, and FM-973.

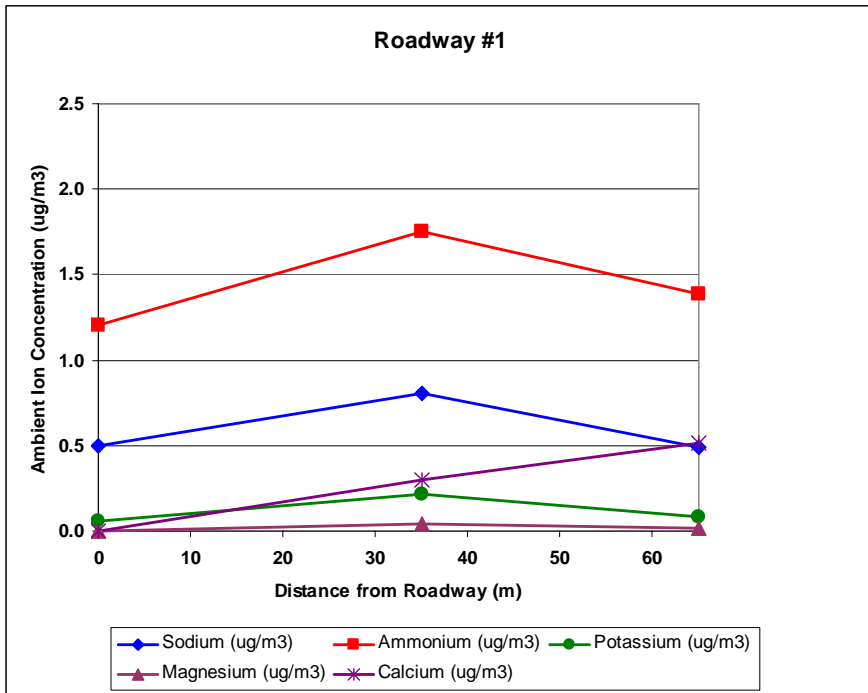
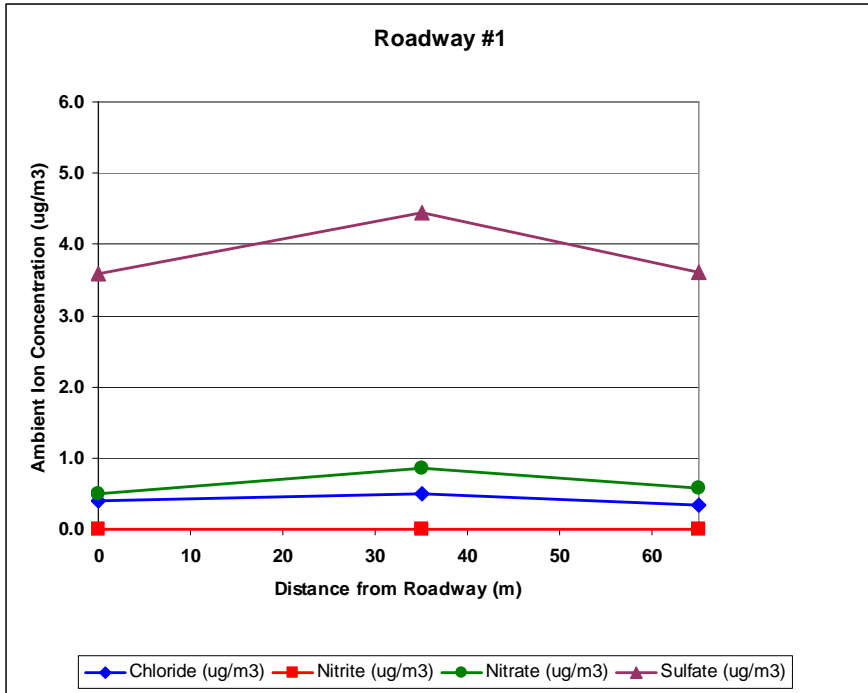


Figure 35. Roadway falloff of ion concentrations near SH-71.

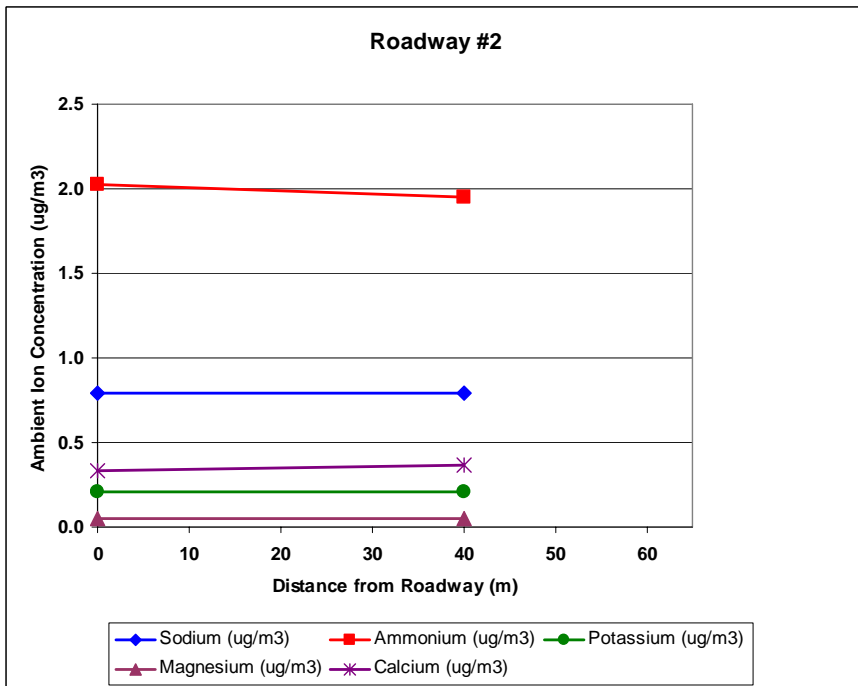
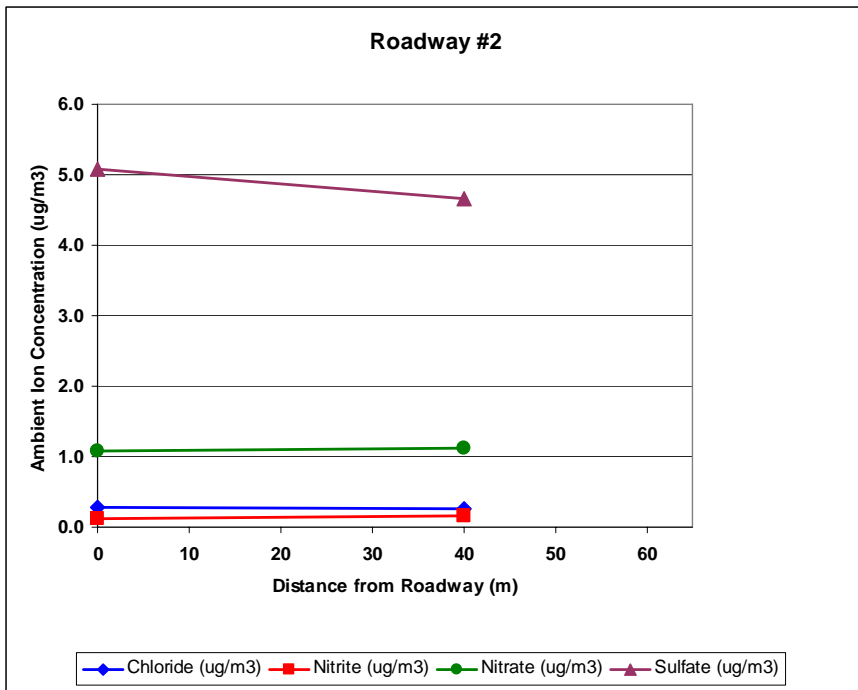


Figure 36. Roadway falloff of ion concentrations near I-35.

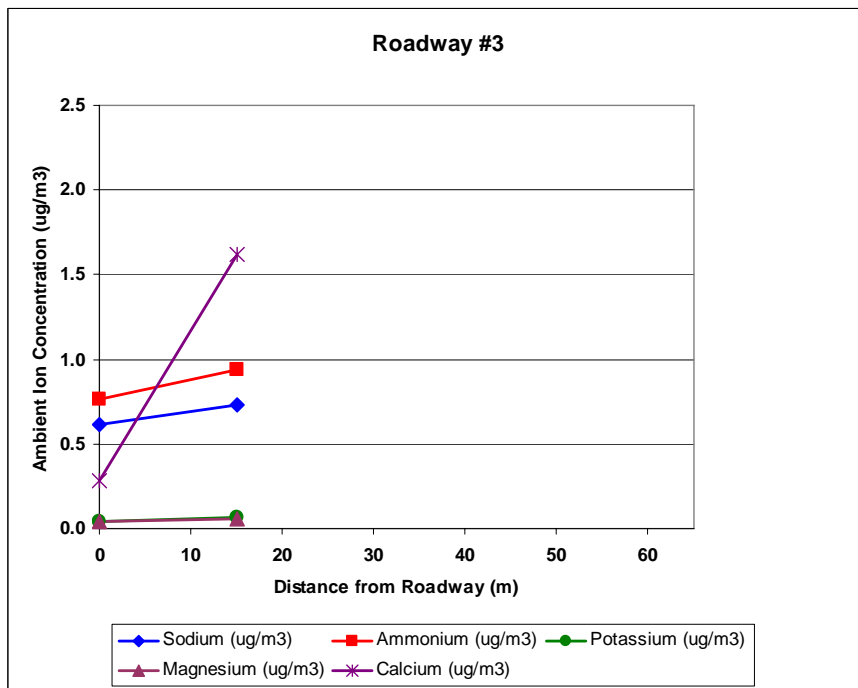
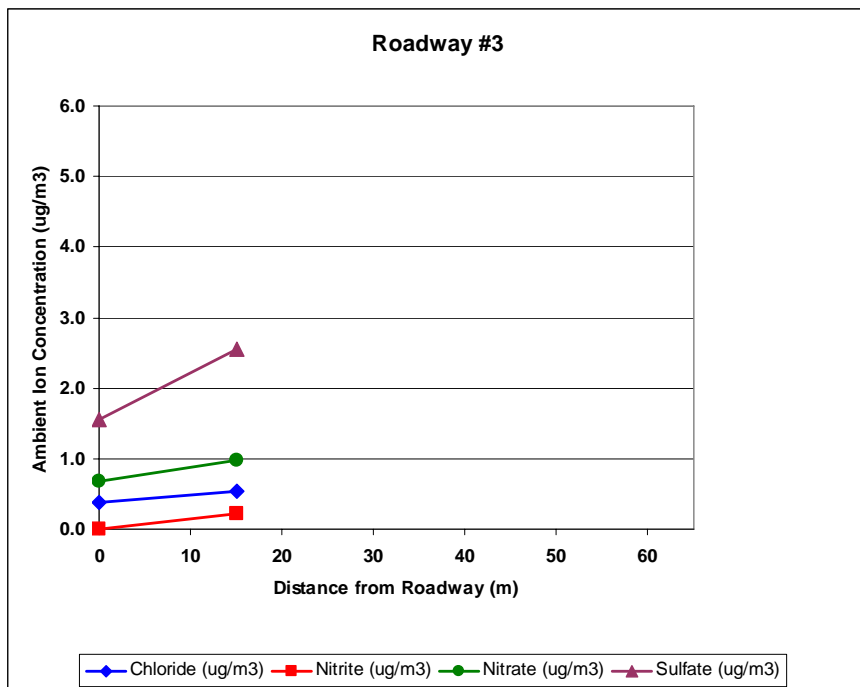


Figure 37. Roadway falloff of ion concentrations near FM-973.

DRAFT

Particle bound organic species

For the SH-71 roadway, three sets of high-volume quartz fiber filters were collected at three locations 80 m upwind, 35 m downwind and 65 m downwind of the center of the road: one each during morning rush hour on April 12, 2007, one each during mid-day and afternoon rush-hour on April 12, 2007 and one each during the morning rush-hour on April 13, 2007. For I-35, two sets of high-volume quartz fiber filters were collected at 110 m upwind on July 11, 2007 during the morning and mid-day, and four sets were collected at 40 m downwind during the morning and mid-day on July 10, 2007 and July 11, 2007. For FM-973, four sets of high-volume quartz fiber filters were collected both at 80m upwind and 15 m downwind of the center of the road: one each during the early afternoon on July 12, 2007, two each during the morning and mid-day of July 13, 2007, and one each during the morning of July 14, 2007.

Particulate organic compounds measured included 10 PAH compounds (Fluoranthene, Pyrene, Chrysene, Benzo(b)fluoranthene/Benzo(k)fluoranthene, Benzo(e)pyrene, Benzo(a)pyrene, Perylene, Indeno(1,2,3-cd)pyrene, Dibenz(a,h)anthracene and Benzo(g,h,i)perylene), 14 alkanes (ranging from C20 to C33 normal alkanes), three petroleum biomarkers (hopane, homohopane and bishomohopane) and 4 sugar compounds (Levoglucon, Glucose, Glycerol, Sucrose). Organic and elemental carbon concentrations and ratios of elemental carbon to total carbon were also measured. Representative falloff curves of the concentration of these classes of organic compounds are shown in Figures 38.

Figure 38 shows the falloff of PAH concentrations from the vicinity of SH-71. PAH concentrations near I-35 and FM-973 were below detection limits. For all plots, concentrations are given in nanograms per cubic meter and the upwind site is plotted at 0 meters downwind of the roadway center even though they may be at varying distances upwind of the roadway. This convention is adopted for clarity in presenting the data.

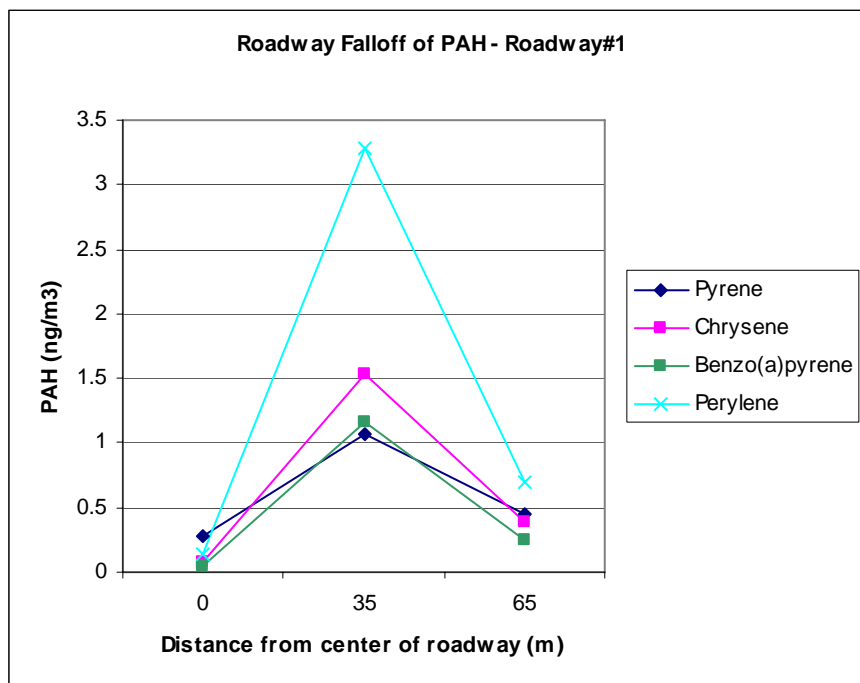


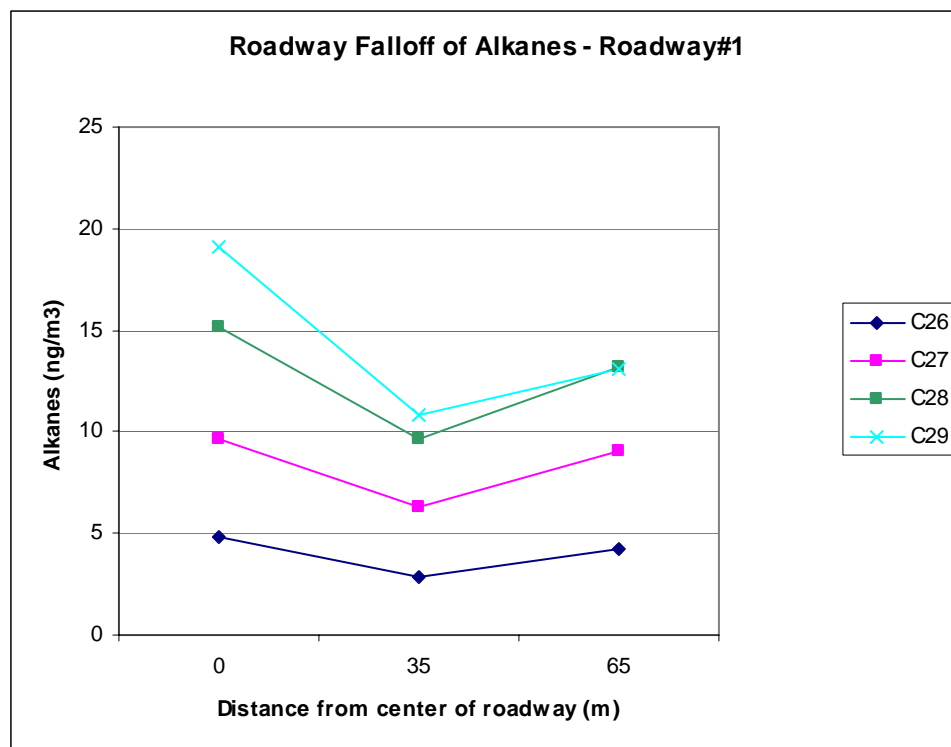
Figure 38. Roadway falloff near SH-71 of four representative particle bound PAH species.

DRAFT

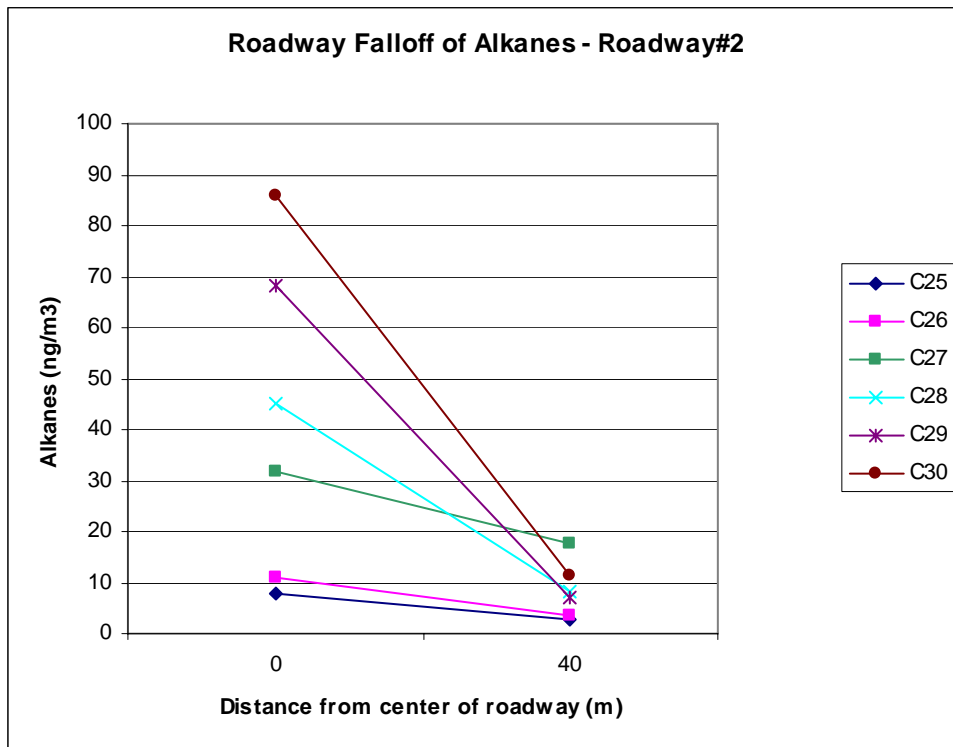
From Figure 38, it is clear that the PAH show classic falloff behavior with low concentrations upwind of the roadway, the greatest concentration immediately downwind of the source, decreasing concentrations further downwind from the roadway. For this class of compounds, it is clear that the roadway is the dominant source of the pollutants. This is consistent with the dominant source of PAH being gasoline powered vehicles.

Figure 39 shows the falloff of concentrations of four representative alkane compounds near SH-71, I-35, and FM-973, respectively. The behavior of this class of compounds is consistent near SH-71: all species show lowest concentrations immediately downwind of the source. However, given that the precision of the GC/MS quantification is $\pm 20\%$, the data are likely equivalent statistically. The falloff of this class of compounds has the opposite behavior near I-35 and FM-973: concentrations are higher upwind of the roadway than downwind. Numerous sources of alkanes have been identified including vegetation waxes, soil material, and combustion processes. From the data, it is clear that either the emissions from the roadway are not the sole source of these species or these semi-volatile species are condensing onto particles emitted by vehicles.

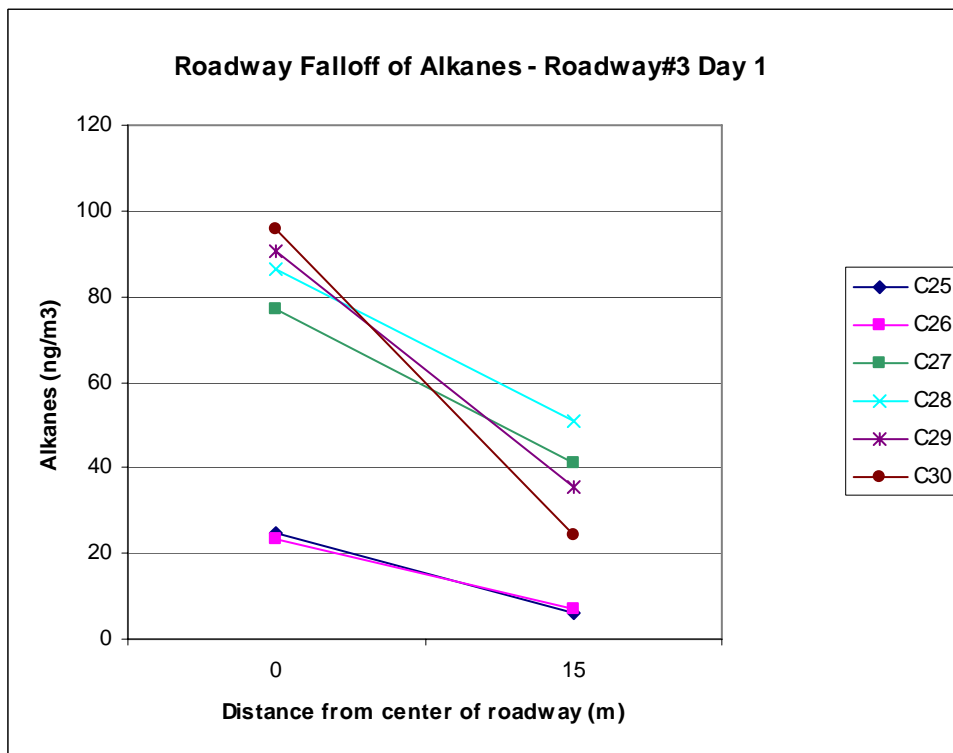
(a)



(b)



(c)



(d)

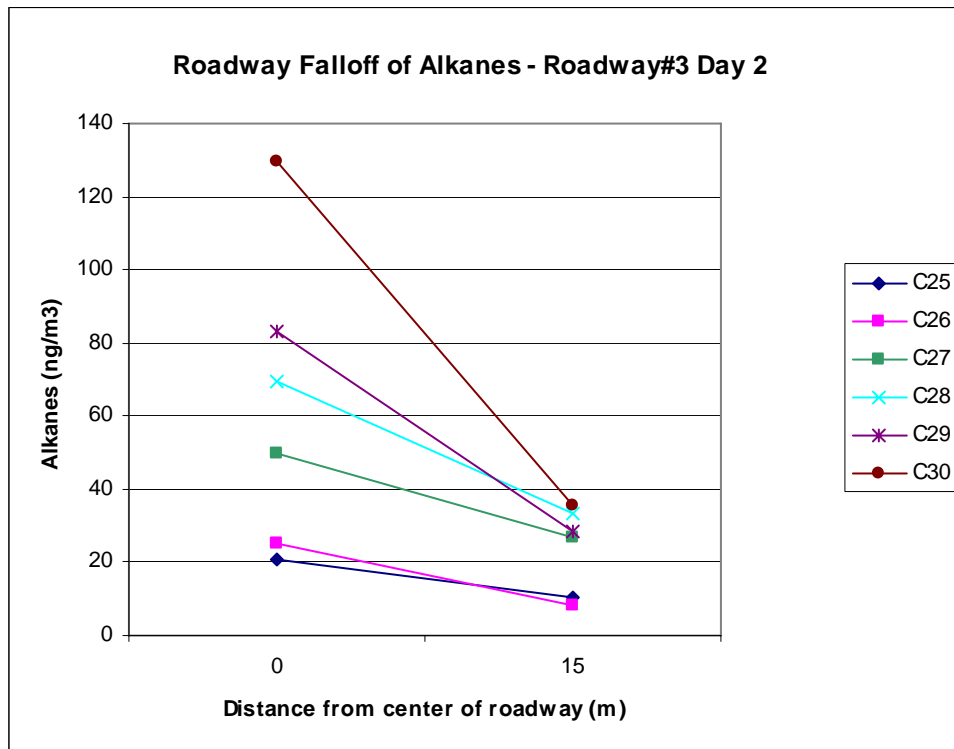


Figure 39. Roadway falloff of four representative alkanes near (a) SH-71, (b) I-35, (c) FM-973 (Day 1: July 12, 2007), (d) and FM-973 (Day 2: July 13, 2007).

DRAFT

Figure 40 shows the concentration of petroleum biomarkers including hopane, homohopane and bishomohopane in the vicinity of SH-71. There is no consistent trend amongst these three compounds. For the parent hopane compound, the highest concentrations are measured immediately downwind of the roadway, but further downwind, hopane was below the detection limits of approximately 0.2 ng m^{-3} . For homohopane and bishomohopane, concentrations upwind of the roadway and immediately downwind are similar, with lower concentrations further downwind of the roadway. Hopane, homohopane, and bishomohopane concentrations near I-35 and FM-973 were below detection limits

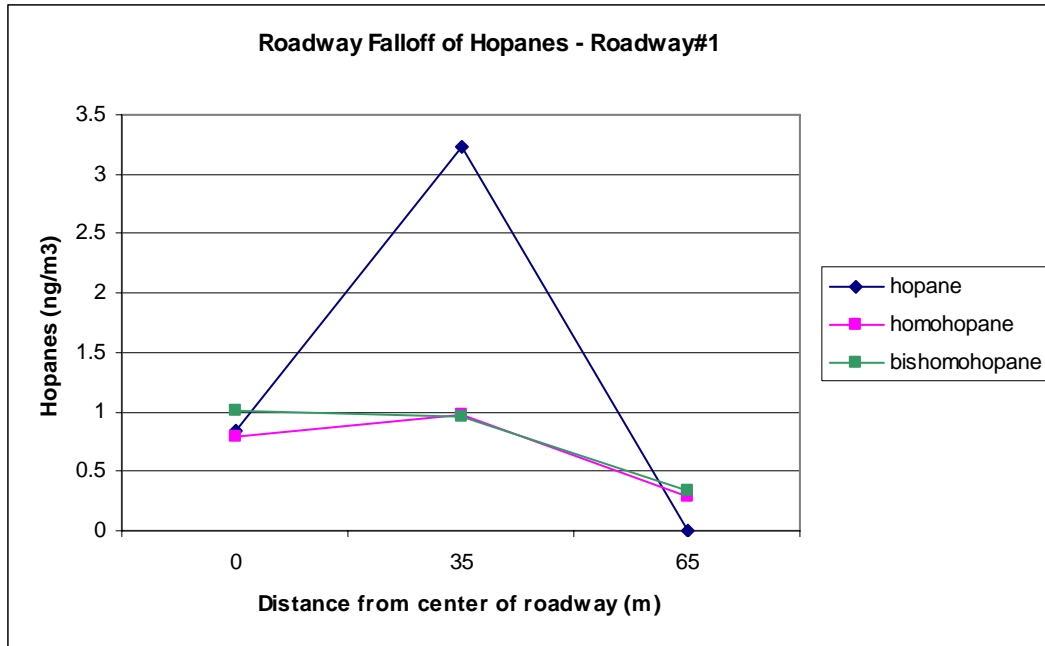


Figure 40. Roadway falloff of four representative hopanes near SH-71.

DRAFT

Figure 41 shows the concentration of two sugar related compounds in the vicinity of the roadway. There is no consistent trend amongst these compounds. Levoglucosan, a marker species for biomass combustion increases going from upwind to downwind locations, while sucrose is relatively constant. Since sucrose is a marker for biological activity in local soils, the trend for sucrose makes sense. However, there were no likely sources for levoglucosan in the vicinity of the sampling during the experiment, so the trend in that compound cannot yet be explained.

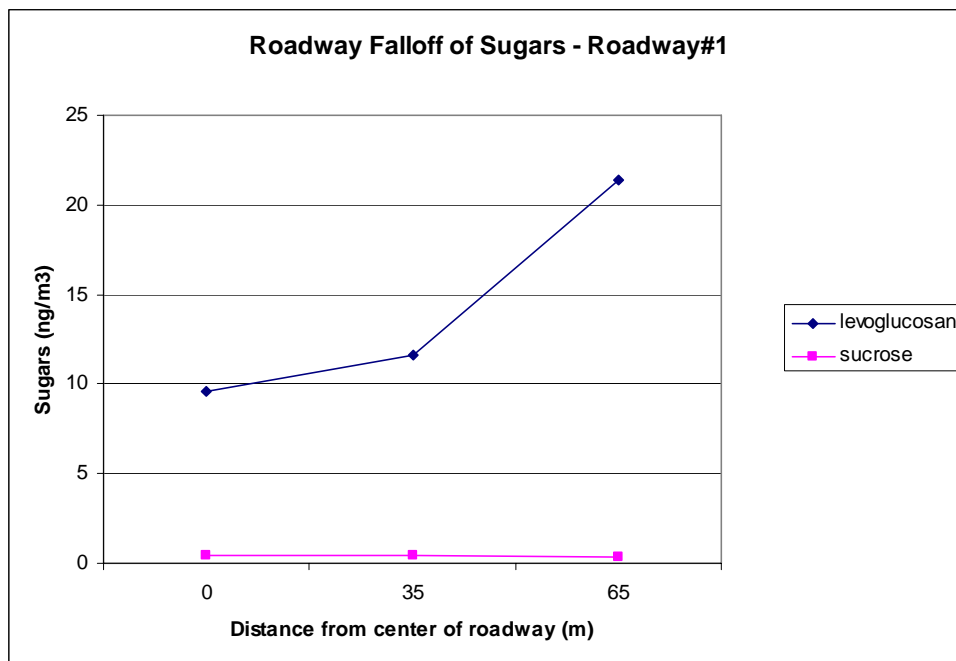


Figure 41. Roadway falloff of four representative sugars near SH-71.

DRAFT

Figure 42 shows the falloff of concentrations of organic and elemental carbon in the vicinity of SH-71, I-35, and FM-973. Figure 43 shows the falloff of ratios of elemental carbon to total carbon in the vicinity of the three roadways. Although trends in organic carbon concentrations are not consistent between roadways, suggesting other sources, ratios of elemental to total carbon exhibit classic falloff behavior with low concentrations upwind of the roadway, the greatest concentration immediately downwind of the source, decreasing concentrations further downwind.

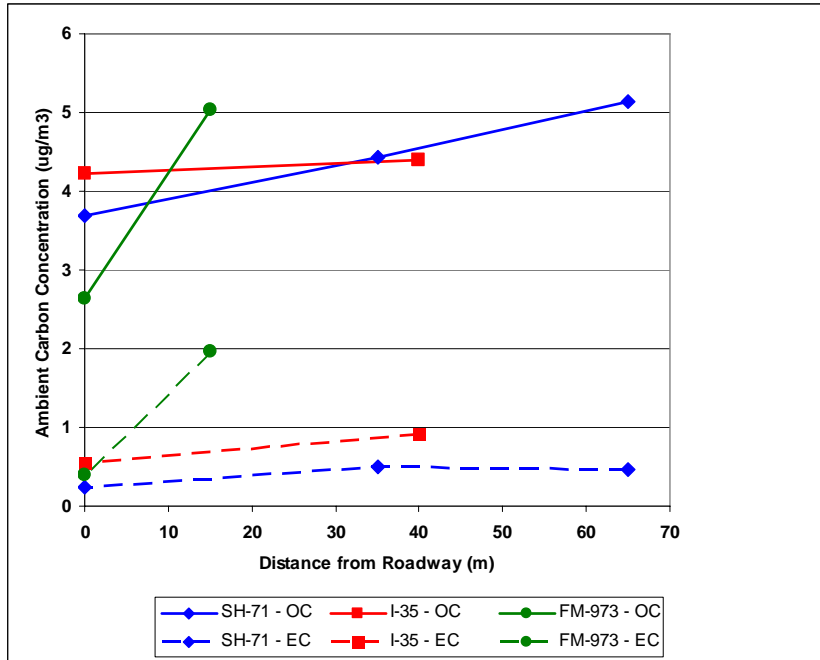


Figure 42. Roadway falloff of organic and elemental carbon near SH-71, I-35, and FM-973.

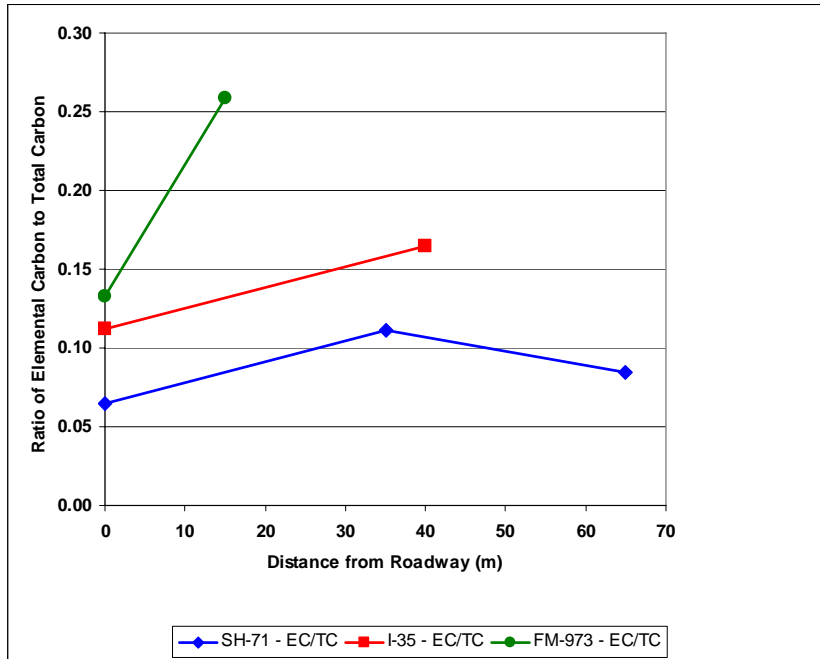


Figure 43. Roadway falloff of ratios of elemental carbon to total carbon near SH-71, I-35, and FM-973.

DRAFT

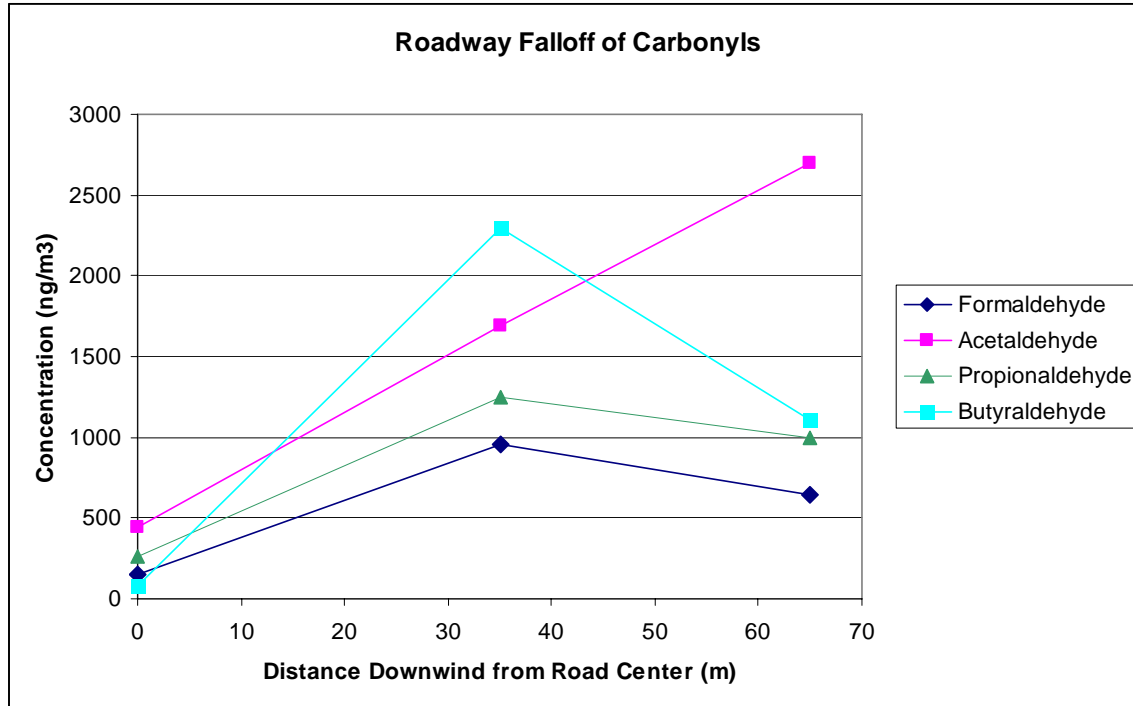
DRAFT

Carbonyls

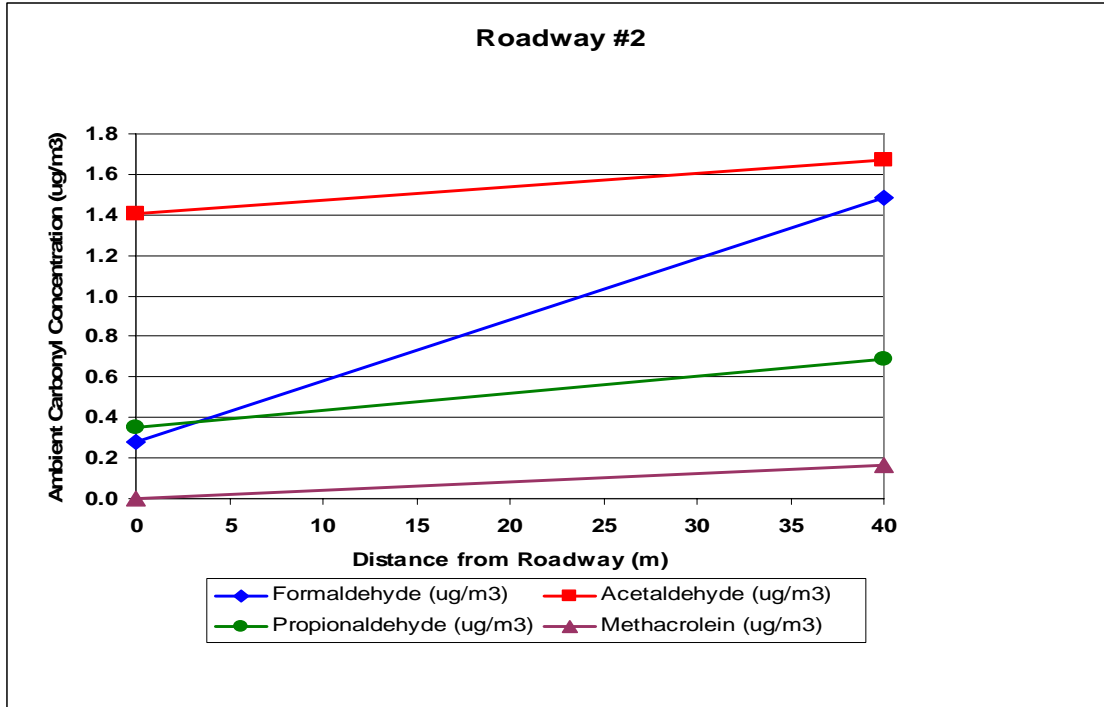
Measurements were taken of nine carbonyl species during four sampling periods over two days at the three stationary sites near SH-71 (80 meters upwind of the center of the roadway and 35 and 65 m downwind), at two sites near I-35 (110 m upwind and 40 m downwind), and at two stationary sites near FM-973 (80m upwind and 15 m downwind).

Ambient concentrations averaged over all sample periods of four of the measured carbonyls are presented in Figure 44. Note that the upwind concentration were measured at various distances upwind of the center of the roadway but are plotted here at a distance of 0 meters for clarity.

(a)



(b)



(c)

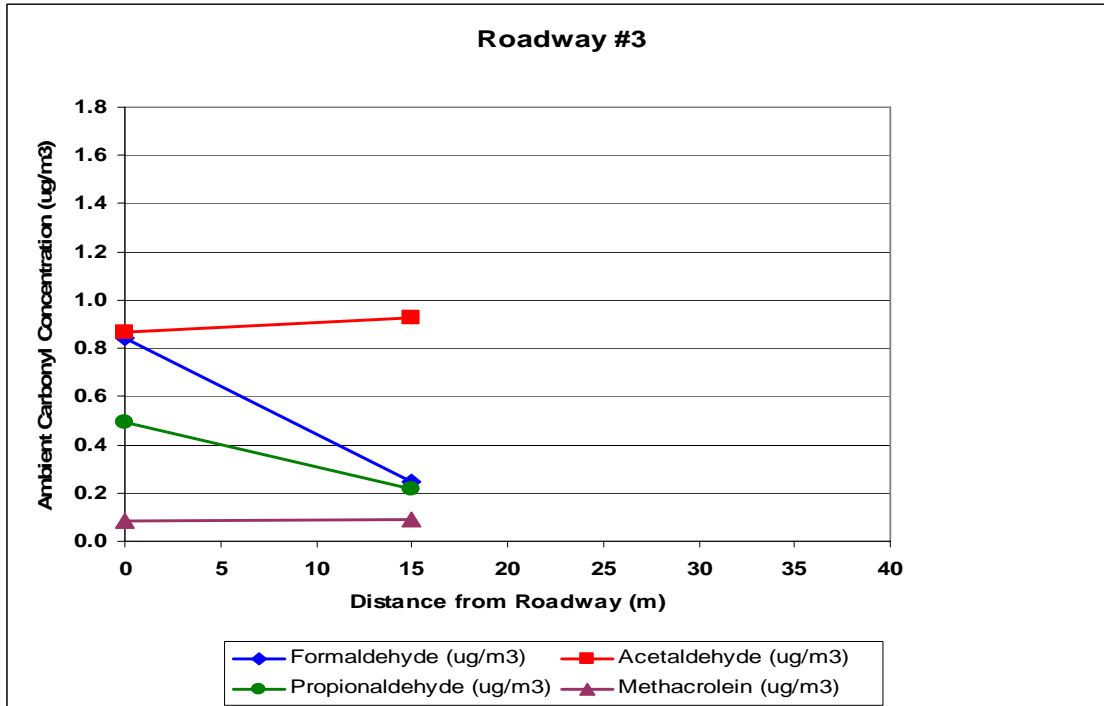


Figure 44. Concentration of four carbonyls vs. distance downwind from (a) SH-71, (b) I-35, and (c) FM-973.

Three of the carbonyls show falloff in concentrations with increased distance downwind of SH-71: formaldehyde, propionaldehyde and butyraldehyde. The falloff in concentration moving

DRAFT

away from the roadway is greater for butyraldehyde (the straight chain C4 aldehyde) than for formaldehyde (C1 aldehyde) or propionaldehyde (C3 aldehyde). Surprisingly, acetaldehyde (C2 aldehyde) increases in concentration at the far downwind site. One possible explanation might be that the formation of acetaldehyde by atmospheric chemistry from reaction of primary emissions from motor vehicles. For all carbonyls, the concentrations at the downwind sites far exceed the upwind concentration near SH-71. Results are similar for I-35. In contrast to I-35 and SH-71, concentrations of carbonyls, with the exception of acetaldehyde, 15 m downwind of FM-973 are lower than concentrations upwind.

DRAFT

Speciated VOC Concentrations

Air samples were collected in polished stainless steel canisters and returned to analytical laboratories at the University of Texas to determine concentrations of hydrocarbons. VOC canister samples were collected on July 31, 2007 for SH-71 and FM-973 and on August 1, 2007 for I-35. Upwind and downwind concentrations of target compounds as well as downwind/upwind ratios at each site are presented in Table 4. Figures 45 through 47 and highlighted rows in Table 4 show upwind and downwind concentrations of selected mobile source air toxics at each site. These species were included in the U.S. EPA's (11) profile for mobile source air toxics trend analysis.

Upwind concentrations near FM-973 are included in Table 4, but were recognized as not representative of actual conditions based on likely contamination from a nearby motor vehicle or generator. Thus, ratios of downwind to upwind concentrations are not presented for this site. Ambient concentrations of most VOCs were 1.1 to 4.5 times downwind of I-35 and SH-71 than upwind. Ambient concentrations of benzene, toluene, ethylbenzene, and xylene isomers (BTEX), specifically, were 2 to 2.5 times higher downwind of I-35 and SH-71 than upwind. Although the range of downwind to upwind VOC *ratios* near I-35 and SH-71 were similar to each other, actual VOC concentrations were consistently higher near SH-71 than near I-35.

Annual average speciated VOC concentrations for 2000 for two ambient monitoring sites, Clinton and Deer Park, in the Houston industrial area, are presented in Table 4 for comparison purposes (12). BTEX concentrations upwind and downwind of the roadways included in this study are lower than or comparable to concentrations at Clinton and Deer Park. Although this trend was similar for most other species, several hydrocarbons, which may be fuel markers, including hexane, 1-pentene, pentane, cis-2-butene, 3-methylpentane were notably higher downwind of the roadway sites than at the industrial sites.

DRAFT

Table 4. Upwind and downwind speciated VOC concentrations and ratios of concentrations at roadway sites. Speciated VOC concentrations at two ambient monitoring sites in the Houston/Galveston industrial area during TexAQS 2000 are presented for reference purposes (Jeffries, 2003). Note: ND=non detect.

Compound	I-35 Upwind (ppbC)	I-35 Down- wind (ppbC)	I-35 Downwind/ Upwind Ratio	SH-71 Upwind (ppbC)	SH-71 Down- wind (ppbC)	SH-71 Downwind/ Upwind Ratio	FM-973 Upwind* (ppbC)	FM-973 Down- wind (ppbC)	Clinton (ppbC)	Deer Park (ppbC)
1,2,4-trimethyl Benzene	0.17	0.11	0.66	0.15	0.20	1.37	0.46	0.35	0.95	0.60
1,3,5-trimethyl Benzene	ND	0.38	-	0.50	0.83	1.66	1.19	0.48	0.64	0.37
1-pentene	ND	1.42	-	2.54	4.51	1.78	8.66	1.64	1.12	
1,3-butadiene	ND	ND	-	ND	ND	-	ND	ND	2.39	0.64
2,2,4-trimethylpentane	1.08	1.19	1.10	1.54	2.43	1.57	3.95	1.71	12.10	1.65
2,2-dimethylbutane	ND	1.06	-	1.54	2.66	1.73	4.25	1.03	0.82	0.50
2,3,4-trimethylpentane	ND	ND	-	ND	0.71	-	1.11	ND	4.85	0.57
2,3-dimethylbutane	0.44	1.18	2.67	2.02	3.84	1.90	7.28	1.28	4.12	1.14
2,3-dimethylpentane	0.16	0.21	1.35	0.52	0.85	1.64	1.39	0.27	1.63	0.58
2,4-dimethylpentane	0.07	0.27	3.77	0.53	0.98	1.84	1.67	0.34	1.99	0.40
2-methyl-1-pentene	ND	ND	-	0.39	1.37	3.46	2.47	ND		
2-methyl-2-butene	1.18	4.40	3.73	8.25	14.71	1.78	26.20	4.87	0.25	0.09
2-methylheptane	ND	ND	-	ND	0.33	-	0.42	ND	1.19	0.40
2-methylhexane	0.45	0.70	1.57	1.37	2.50	1.83	4.16	0.88	2.05	0.89
2-methylpentane	2.96	5.21	1.76	8.46	16.18	1.91	29.69	5.36	7.05	3.58
3-methyl-1-butene	ND	ND	-	1.14	2.10	1.84	4.12	0.68		
3-methylheptane	ND	ND	-	ND	0.43	-	0.69	ND	0.92	0.44
3-methylhexane	0.32	0.78	2.48	1.34	2.44	1.83	3.77	0.96	2.88	1.33
3-methylpentane	0.99	2.82	2.86	5.00	8.98	1.80	16.39	3.27	4.18	2.26
Acetylene	0.55	2.53	4.57	0.65	0.69	1.06	0.60	1.13	2.93	2.70
a-pinene	0.64	ND	-	0.55	1.11	2.00	ND	ND		
Benzene	1.01	2.15	2.13	2.11	4.02	1.91	5.76	1.99	5.28	3.37
Butane	4.65	13.11	2.82	24.16	43.53	1.80	94.75	14.78		
Cis-2-butene	ND	1.39	-	2.39	4.62	1.93	8.92	1.53	1.84	0.34

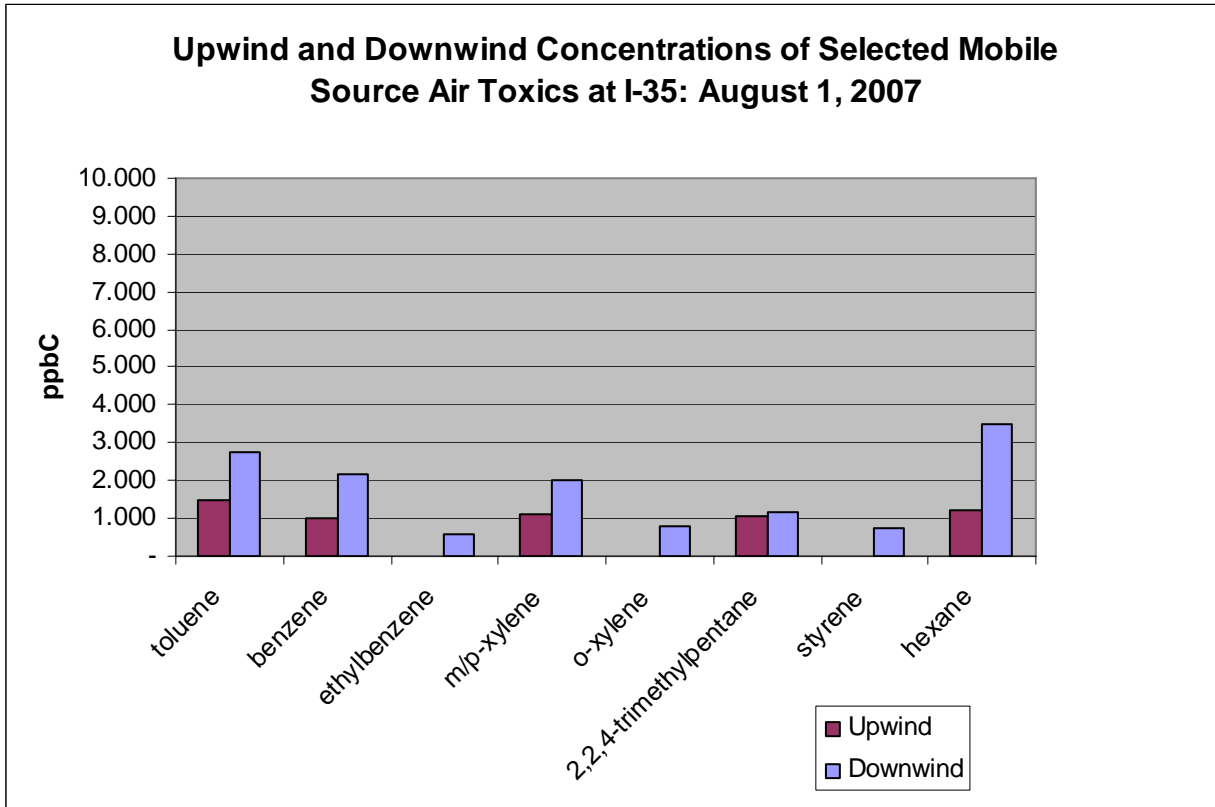
DRAFT

Cis-2-hexene	ND	ND	-	ND	0.52	-	0.84	ND		
Cis-2-pentene	0.42	1.60	3.80	3.04	5.26	1.73	9.93	1.81	0.89	0.25
Cyclohexane	ND	ND	-	0.57	1.00	1.76	1.64	0.47	1.55	1.25
Cyclopentane	0.58	1.33	2.32	2.21	4.06	1.84	7.73	1.50	1.14	0.59
Cyclopentene	ND	0.59	-	1.30	2.11	1.62	3.49	0.66	0.22	0.12
Ethane	2.94	3.00	1.02	4.25	2.84	0.67	2.62	2.96	21.78	25.35
ethylbenzene	ND	0.59	-	0.72	1.66	2.29	2.02	0.75		
ethylene	0.78	2.44	3.13	0.76	1.18	1.56	0.94	1.76	6.25	13.42
heptane	0.33	0.48	1.47	1.15	1.68	1.46	2.54	0.69	3.20	1.40
hexane	1.23	3.49	2.83	4.93	8.73	1.77	15.75	4.05	6.15	4.51
isobutane	1.22	2.01	1.64	3.59	5.71	1.59	12.31	2.15	20.94	14.68
isopentane	9.72	31.32	3.22	54.64	101.21	1.85	206.76	34.54	35.34	12.16
isoprene	4.30	3.36	0.78	4.18	3.77	0.90	0.78	0.57	1.45	0.84
m/p-xylene	1.13	2.03	1.80	2.61	5.52	2.12	6.66	2.44	6.06	2.67
methylcyclohexane	ND	0.48	-	0.85	1.52	1.79	2.07	0.56		
methylcyclopentane	0.65	1.75	2.67	3.03	5.75	1.90	10.11	2.04	2.79	1.86
nonane	ND	ND	-	ND	ND	-	0.46	ND	0.85	0.32
n-propylbenzene	0.35	ND	-	ND	0.50	-	0.79	ND	0.42	0.24
octane	ND	ND	-	ND	0.59	-	0.69	0.46		
o-xylene	ND	0.81	-	1.02	1.98	1.95	2.51	0.98	2.05	1.14
pentane	4.56	13.16	2.89	22.81	42.29	1.85	82.81	15.34	14.06	5.45
propane	2.92	2.11	0.72	2.37	1.88	0.79	1.84	1.71	24.59	25.19
propylene	ND	1.03	-	ND	0.63	-	0.63	0.84	8.19	23.34
styrene	ND	0.77	-	0.87	0.79	0.90	0.91	1.16	1.22	0.65
toluene	1.48	2.76	1.87	3.35	6.53	1.95	8.81	3.13	13.60	6.63
trans-2-butene	ND	ND	-	ND	6.34	-	8.40	ND	2.40	0.44
trans-2-hexene	ND	0.20	-	0.36	1.32	3.68	2.89	0.25		
trans-2-pentene	0.77	3.00	3.90	5.63	10.04	1.78	18.51	3.46	1.70	0.47
Total:Target	48.02	117.21		189.36	345.35		643.31	126.81		
Total: Non-Target	40.58	69.28		84.80	126.85		204.40	76.67		
Total	88.60	186.49		274.16	472.21		847.70	203.49	328.4	189.3

*This sample is included for the sake of completeness, but was judged to be not representative of actual upwind conditions based on likely contamination from a nearby motor vehicle or generator.

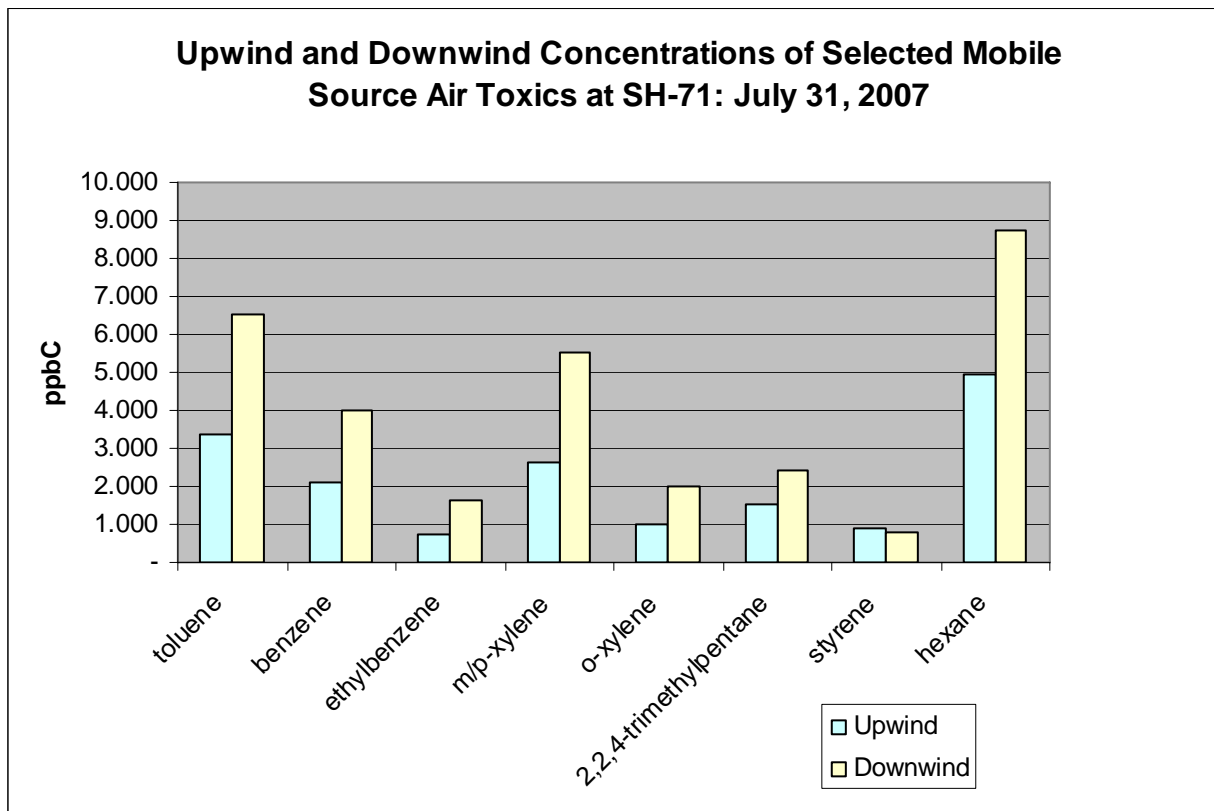
DRAFT

Figure 45. Upwind and downwind concentrations of selected mobile source air toxics detected at I-35 on August 1, 2007.



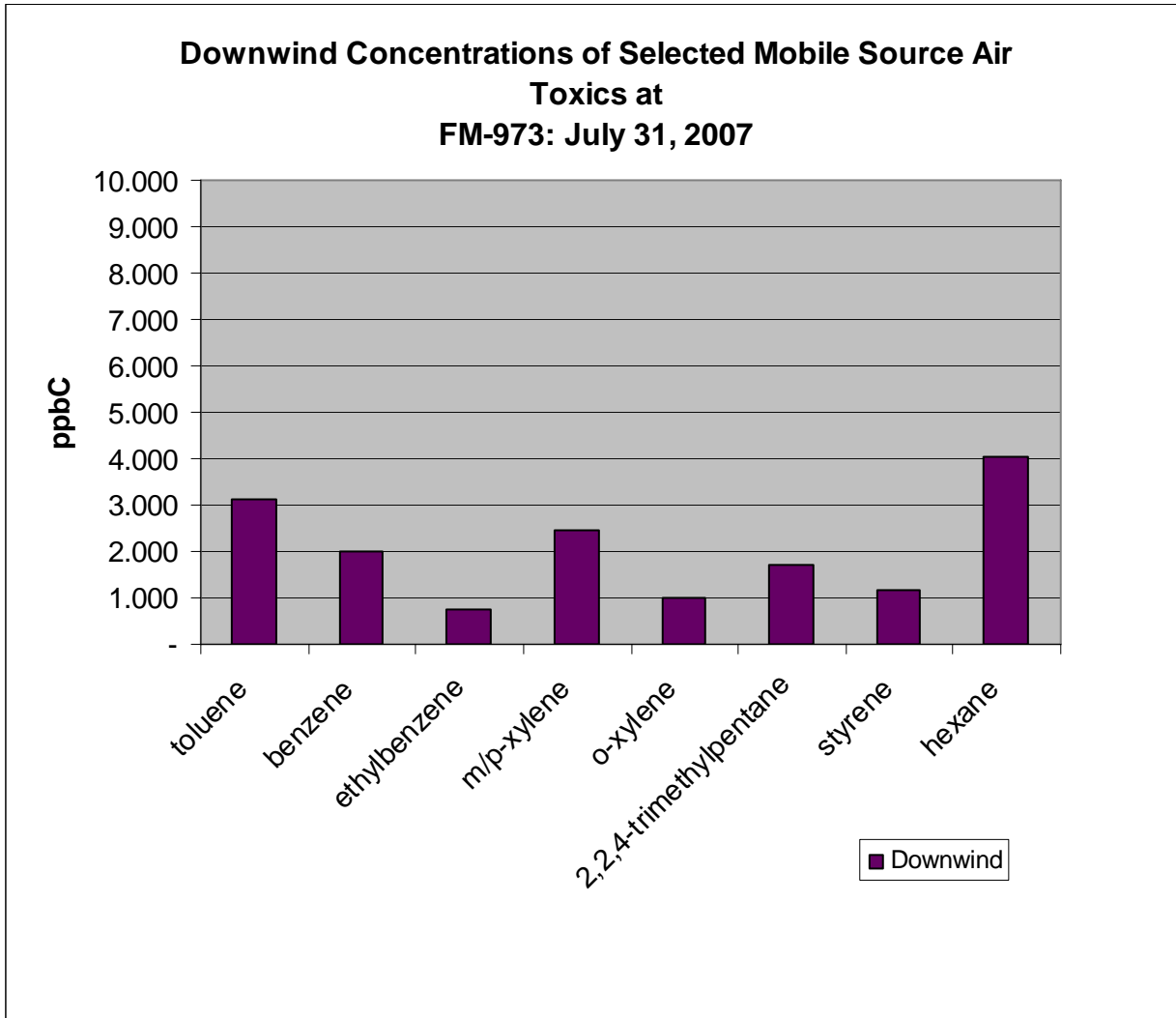
DRAFT

Figure 46. Upwind and downwind concentrations of selected mobile source air toxics detected at SH-71 on July 31, 2007.



DRAFT

Figure 47. Upwind and downwind concentrations of selected mobile source air toxics detected at FM-973 on July 31, 2007.



DRAFT

References

- (1) Zhu, Y.F., Hinds, W.C., Kim, S., Shen, S. and Sioutas, C. Study of ultrafine particles near a major highway with heavy-duty diesel traffic. *Atmospheric Environment* **2002**, *36*, 4323-4335.
- (2) Gramotnev, G. and Ristovski, Z. Experimental investigation of ultra-fine particle size distribution near a busy road. *Atmospheric Environment* **2004**, *38*, 1767-1776.
- (3) Reponen, T., Grinshpun, S.A., Trakumas, S., Martuzevicius, D., Wang, Z., LeMasters, G., Lockey, J.E. and Biswas, P. Concentration gradient patterns of aerosol particles near interstate highways in the Greater Cincinnati airshed. *Journal of Environmental Monitoring* **2003**, *5*, 557-562.
- (4) Zhu, Y.F., Kuhn, T., Mayo, P. and Hinds, W.C. Comparison of daytime and nighttime concentration profiles and size distributions of ultrafine particles near a major highway. *Env. Sci. Tech.*, **2006**, *40*, 2531-2536.
- (5) Kittelson, D. B. Engines and Nanoparticles: A Review. *Journal of Aerosol Science* **1998**, *29*, 575-588.
- (6) Morawska, L.; Bofinger, N. D.; Kocis, L.; Nwankwoala, A. Submicrometer and Supermicrometer Particles from Diesel Vehicle Emissions. *Environmental Science and Technology* **1998**, *32*, 2033-2042.
- (7) Abu-Allaban, M.; Coulomb, W.; Gertler, A. W.; Gillies, J.; Pierson, W. R.; Rogers, C. F.; Sagebiel, J. C.; Tarnay, L. Exhaust Particle Size Distribution Measurements at the Tuscarora Mountain Tunnel. *Aerosol Science and Technology* **2002**, *36*, 771-789.
- (8) Zhu, Y. F.; Eiguren-Fernandez, A.; Hinds, W. C.; Miguel, A. H. In-cabin commuter exposure to ultrafine particles on Los Angeles freeways. *Environmental Science & Technology* **2007**, *41*, 2138-2145.
- (9) Pirjola, L.; Paasonen, P.; Pfeiffer, D.; Hussein, T.; Hameri, K.; Koskentalo, T.; Virtanen, A.; Ronkko, T.; Keskinen, J.; Pakkanen, T. A.; Hillamo, R. E. Dispersion of particles and trace gases nearby a city highway: Mobile laboratory measurements in Finland. *Atmospheric Environment* **2006**, *40*, 867-879.
- (10) Westerdahl, D.; Fruin, S.; Sax, T.; Fine, P. M.; Sioutas, C. Mobile platform measurements of ultrafine particles and associated pollutant concentrations on freeways and residential streets in Los Angeles. *Atmospheric Environment* **2005**, *39*, 3597-3610.
- (11) United States Environmental Protection Agency, Regulatory Impact Analysis, Control of Hazardous Air Pollutants from Mobile Sources: Chapter 3 Air Quality and Resulting Health and Welfare Effects of Air Pollution from Mobile Sources, Assessment and Standards Division Office of Transportation and Air Quality, U.S. Environmental Protection Agency, EPA-420-R-07-002, February 2007.

DRAFT

- (12) Jeffries, H, personal communication, October 2003.

DRAFT

Appendix A.
 Austin Roadway Sampling Project
 Low-volume filter samples
 Sample Location, Date, and Time

**Roadway #1 - US-71
 Far Downwind**

Filter Number	Ambient Sampling Start Date	Ambient Sampling Start Time	Ambient Sampling End Date	Ambient Sampling End Time	Total Sampling Time (hr)	Total Sampling Time (min)
P6054373	4/12/2007	10:56	4/12/2007	14:56	4:00	240
P6025540	4/12/2007	14:56	4/12/2007	18:56	4:00	240
P6025539	4/13/2007	8:57	4/13/2007	12:57	4:00	240

Near Downwind

Filter Number	Ambient Sampling Start Date	Ambient Sampling Start Time	Ambient Sampling End Date	Ambient Sampling End Time	Total Sampling Time (hr)	Total Sampling Time (min)
P6025527	4/12/2007	6:40	4/12/2007	10:40	4:00	240
P6024925	4/12/2007	10:50	4/12/2007	14:50	4:00	240
P6024924	4/12/2007	14:50	4/12/2007	18:50	4:00	240
P6024923	4/12/2007	18:50	4/12/2007	22:50	4:00	240
P6024922	4/12/2007	22:50	4/13/2007	2:50	4:00	240
P6024921	4/13/2007	8:15	4/13/2007	12:15	4:00	240
P6024920	4/13/2007	12:15	4/13/2007	13:38	1:23	83

Upwind

Filter Number	Ambient Sampling Start Date	Ambient Sampling Start Time	Ambient Sampling End Date	Ambient Sampling End Time	Total Sampling Time (hr)	Total Sampling Time (min)
P6025502	4/12/2007	10:00	4/12/2007	14:21	4:21	261
P6025548	4/12/2007	14:40	4/12/2007	18:40	4:00	240
P6025547	4/12/2007	18:40	4/12/2007	22:40	4:00	240
P6025545	4/13/2007	7:40	4/13/2007	11:40	4:00	240
P6025544	4/13/2007	11:40	4/13/2007	12:46	1:06	66

**Roadway #2 - North I-35
 Downwind**

Filter Number	Ambient Sampling Start Date	Ambient Sampling Start Time	Ambient Sampling End Date	Ambient Sampling End Time	Total Sampling Time (hr)	Total Sampling Time (min)
P6054362	7/10/2007	12:00	7/10/2007	16:00	4:00	240
P6054361	7/10/2007	16:00	7/10/2007	20:00	4:00	240
P6054353	7/11/2007	6:11	7/11/2007	10:00	3:49	229

DRAFT

P6054351	7/11/2007	10:02	7/11/2007	14:00	3:58	238
P6054354	7/11/2007	14:01	7/11/2007	18:00	3:59	240

Upwind

Filter Number	Ambient Sampling Start Date	Ambient Sampling Start Time	Ambient Sampling End Date	Ambient Sampling End Time	Total Sampling Time (hr)	Total Sampling Time (min)
P6054380	7/10/2007	12:00	7/10/2007	16:00	4:00	240
P6054369	7/11/2007	6:26	7/11/2007	10:00	3:34	214
P6054368	7/11/2007	10:00	7/11/2007	14:00	4:00	240
P6054366	7/11/2007	14:12	7/11/2007	18:00	3:48	228

Roadway #3 - FM 973

Downwind

Filter Number	Ambient Sampling Start Date	Ambient Sampling Start Time	Ambient Sampling End Date	Ambient Sampling End Time	Total Sampling Time (hr)	Total Sampling Time (min)
P6054365	7/12/2007	14:00	7/12/2007	18:00	4:00	240
P6054376	7/13/2007	8:00	7/13/2007	12:00	4:00	240
P6054357	7/13/2007	12:06	7/13/2007	16:00	3:54	234
P6054363	7/13/2007	16:00	7/13/2007	18:07	2:07	127
P6054390	7/14/2007	8:00	7/14/2007	11:36	3:36	127

Upwind

Filter Number	Ambient Sampling Start Date	Ambient Sampling Start Time	Ambient Sampling End Date	Ambient Sampling End Time	Total Sampling Time (hr)	Total Sampling Time (min)
P6054352	7/12/2007	14:00	7/12/2007	18:00	4:00	240
P6054358	7/13/2007	8:00	7/13/2007	12:00	4:00	240
P6054359	7/13/2007	12:00	7/13/2007	16:00	4:00	240
P6054392	7/13/2007	16:07	7/13/2007	18:14	2:07	127
P6054360	7/14/2007	8:00	7/14/2007	12:00	4:00	240

Blanks

Filter Number	Ambient Sampling Start Date	Ambient Sampling Start Time	Ambient Sampling End Date	Ambient Sampling End Time	Total Sampling Time (hr)	Total Sampling Time (min)
P6054379						
P6054355						
P6054378						
P6054367						
P6054377						